ELSEVIER

International Journal of Solids and Structures 41 (2004) 1285–1311

INTERNATIONAL JOURNAL OF SOLIDS and STRUCTURES

www.elsevier.com/locate/ijsolstr

A Galerkin boundary integral method for multiple circular elastic inclusions with uniform interphase layers

S.G. Mogilevskaya *, S.L. Crouch

Department of Civil Engineering, University of Minnesota, 500 Pillsbury Drive S.E., Minneapolis, MN 55455 0116, USA

Received 17 June 2003; received in revised form 22 September 2003

Abstract

The paper presents a numerical method for solving the problem of an infinite, isotropic elastic plane containing a large number of randomly distributed circular elastic inclusions with uniform interphase layers. The bonds between the inclusions and the interphases as well as between the interphases and the matrix are assumed to be perfect. In general, the inclusions may have different elastic properties and sizes; the thicknesses of the interphases and their elastic properties are arbitrary. The analysis is based on a numerical solution of a complex singular integral equation with the unknown tractions at each circular boundary approximated by a truncated complex Fourier series. The Galerkin technique is used to obtain a system of linear algebraic equations. The resulting numerical method allows one to calculate the elastic fields everywhere in the matrix and inside the inclusions and the interphases. Using the assumption of macro-isotropic behavior in a plane section one can find the effective elastic moduli for an equivalent homogeneous material. The method can be viewed as an extension of our previous work (Int. J. Solids Struct. 39 (2002) 4723) where simpler spring-like interface conditions were modeled. The problem of overlapping of the fibers and matrix inherent to spring type interface is discussed in the context of the present model. Numerical examples are included to demonstrate the effectiveness of the new approach.

Keywords: Galerkin boundary integral method; Complex singular integral equation; Multiple circular inclusions; Uniform interphases

1. Introduction

This paper is concerned with two-dimensional modeling of multiple nonoverlapping circular inclusions (fibers) with uniform interphases. Fiber-reinforced composite materials are a natural and important application of this model. We idealize the fibers as uniform, infinite circular cylindrical inclusions that are connected to the matrix through uniform coaxial bands or interphases. The elastic properties of the interphases are different from those of the fibers and the matrix.

There are several reasons why interphases are present in fiber-reinforced composites. In some materials interphases are the result of coating of the fibers with soft polymers in order to reduce high stresses at the

* Corresponding author. Tel.: +1-612-625-4810; fax: +1-612-626-7750.
E-mail address: mogil003@umn.edu (S.G. Mogilevskaya).

0020-7683/$ - see front matter © 2003 Elsevier Ltd. All rights reserved.
doi:10.1016/j.ijsolstr.2003.09.037

fiber–matrix interfaces and enhance the toughness of the composite (Crasto et al., 1988; Subramanian and Crasto, 1986; Mascia et al., 1993; Nassehi et al., 1993a,b). The interphases may also appear as a result of damage around the fibers in forms of voids, micro-cracks, and other defects (Theocaris, 1987). They may also appear due to chemical reaction or diffusion during the manufacturing process (Lagache et al., 1994; Lutz and Zimmerman, 1996). In any case, the presence of interphases significantly affects the properties of composite materials and needs to be taken into account in numerical modeling.

Numerous papers have been written on the effects of interphases on the micro- and macro-mechanical behavior of fiber-reinforced composite materials (see, for example, Aboudi, 1987; Achenbach and Zhu, 1989, 1990; Benveniste et al., 1989; Benveniste and Miloh, 2001; Bigoni et al., 1998; Bigoni and Movchan, 2002; Christensen and Lo, 1979; Hashin, 1990, 2002; Jasiuk and Kouider, 1993; Theocaris, 1987). Analytical and semi-analytical treatments of the problem are limited to the cases of a single inclusion or a pair of inclusions (Kouris, 1993; Ru, 1998, 1999; Ru and Schiavone, 1997; Sudak et al., 1999; Sudak and Mioduchowski, 2002). The finite element method is the most common numerical tool for modeling fiber-reinforced composites with imperfect interphases (Nassehi et al., 1993a,b; Lagache et al., 1994; Al-Ostaz and Jasiuk, 1996; Wacker et al., 1998) and has been used to model both uniform (Al-Ostaz and Jasiuk, 1996; Lagache et al., 1994) and nonuniform (Wacker et al., 1998) interphases. To avoid large numbers of degrees of freedom in the modeling, these authors employ the concept of a unit cell, but even with this assumption the method is computationally intense, especially for problems involving inclusions with thin interphases.

Boundary element simulations of composite materials with interphases are rather limited. The most common approach is to use the simplest case of a spring type interphase (Achenbach and Zhu, 1989, 1990; Zhu and Achenbach, 1991; Gulrajani and Mukherjee, 1993; Pan et al., 1998). In such a model the thickness of the interphase is neglected, tractions are assumed continuous across the interphase, and the jumps of the normal and shear displacements are taken proportional to the corresponding components of tractions. Hashin (1990, 1991) showed that the spring type model corresponds to the case of a very thin and soft interphase and developed relationships between the interface parameters for the spring type model and the elastic properties of the interphase layer. Benveniste and Miloh (2001) showed that the spring type interphase represents just one of several other possible interphase regimes. They proved that in case of a thin interphase there are seven distinct regimes of interface conditions. Apart from a lack of generality, a disadvantage of the simple spring type model is that it may cause physically unrealistic overlapping of the fibers and matrix under some loading conditions. To prevent overlapping a special iterative procedure needs to be used (Achenbach and Zhu, 1989, 1990). All of the boundary element simulations mentioned above used a unit cell approach and a periodic distribution of the fibers.

To our knowledge, the only boundary element paper where the interphase was regarded as an elastic layer is the one by Liu et al. (2000). They presented a direct boundary element approach for cylindrical and square unit cell models of the composites. The unit cell contained just one inclusion.

In a previous paper (Mogilevskaya and Crouch, 2002) we presented a new approach for solving two-dimensional problems involving a large number of circular elastic inclusions with spring type interface conditions. A similar approach has also been used for problems with multiple perfectly bonded inclusions and holes (Mogilevskaya and Crouch, 2001; Wang et al., 2003, in press). The analysis is based on a numerical solution of a complex hypersingular integral equation with the unknown displacement discontinuities and tractions at each circular boundary approximated by a truncated complex Fourier series (a real variables analog of this approach is presented in Crouch and Mogilevskaya (2003)). Infinite Fourier series, in fact, provide the analytic solution for this class of problems; the only errors introduced in the numerical model are due to truncation of the series and round-off. In the present paper we extend this general approach to the problem of an infinite, isotropic elastic plane containing a large number of randomly distributed circular elastic inclusions with uniform interphase layers. The bonds between the inclusions and the interphases as well as between the interphases and the matrix are assumed to be perfect.

The inclusions may have different elastic properties and sizes and the thicknesses of the interphases and their elastic properties are also arbitrary. The approach allows one to calculate elastic fields everywhere in the matrix and inside the inclusions and the interphases.

2. Problem formulation

Consider an infinite, isotropic elastic plane subjected to a biaxial stress field at infinity and containing N circular elastic inclusions (Fig. 1). The inclusions are connected to the matrix through coaxial circular interphase layers. The bonds between the inclusions and the interphases as well as between the interphases and the matrix are assumed to be perfect. The shear moduli μ_{1j} and Poisson's ratios ν_{1j} $j = 1, \ldots, N$, of the inclusions are arbitrary and are in general different from those of the matrix μ and ν or of the interphases μ_{2j} and ν_{2j}, $j = 1, \ldots, N$. The distances between the inclusions can be arbitrarily small (in particular, their interphases may touch one another). Let R_{1j} and L_{1j} denote the radius and boundary of the jth inclusion, and let R_{2j} and L_{2j} be the radius and boundary of the jth interphase. The center of the inclusion and its interphase is located at the same point z_j. The direction of travel is counterclockwise for all the boundaries L_{1j} and L_{2j}. The unit normal n points to the right of the direction of travel; the unit tangent s is directed in the direction of travel. The distribution of displacements and stresses in the composite solid are to be determined.

The system of inclusions is in equilibrium and it follows that the resultant force and moment on the boundary of each inclusion ($j = 1, \ldots, N$) and interphase are equal to zero. The mathematical expressions for these conditions can be written as follows (Muskhelishvili, 1959)

$$\int_{L_{kj}} \sigma_{kj}(\tau)\,\mathrm{d}\tau = 0, \quad k = 1, 2 \tag{1}$$

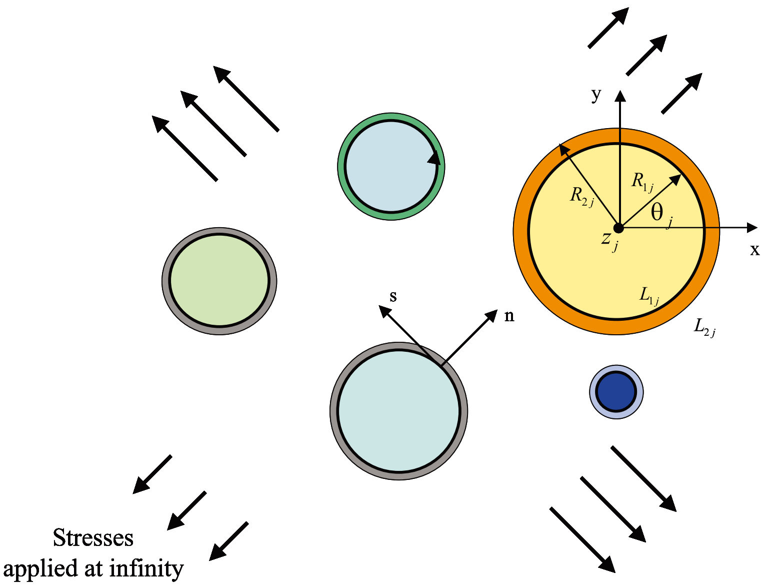

Fig. 1. Problem formulation.

$$\mathrm{Re}\int_{L_{kj}} \tau\overline{\sigma_{kj}(\tau)}\,\mathrm{d}\bar{\tau} = 0, \quad k = 1, 2 \tag{2}$$

where $\sigma_{kj}(z) = \sigma_{kjn}(z) + \mathrm{i}\sigma_{kjs}(z)$, in which $\sigma_{kjn}(z)$ and $\sigma_{kjs}(z)$ are the normal and shear tractions on contour L_{kj}, $z = x + \mathrm{i}y$ is complex coordinate of a point (x, y) in the global Cartesian coordinate system (xOy) in a plane, and $\mathrm{i} = \sqrt{-1}$.

3. Boundary integral equation

As in our previous papers (Mogilevskaya and Crouch, 2001, 2002; Wang et al., 2003, in press) we use the complex hypersingular boundary integral equation originally developed by Linkov and Mogilevskaya (1994), which is valid for the more general problem of an infinite plane or a finite body containing cracks, cavities, and inclusions of arbitrary shapes. For the particular case considered here, the terms containing hypersingular integrals (these involve displacement discontinuities on the boundaries L_{kj}, $k = 1, 2$) vanish and the equation is singular. The resulting equation can be written as follows

$$\sum_{j=1}^{N}\sum_{k=1}^{2}\left[(2a_{1kj} - a_{3kj})\int_{L_{kj}}\frac{\sigma_{kj}(\tau)\,\mathrm{d}\tau}{\tau - t} + (a_{1kj} - a_{3kj})\int_{L_{kj}}\sigma_{kj}(\tau)\frac{\partial}{\partial t}K_1(\tau, t)\,\mathrm{d}\tau + a_{1kj}\int_{L_{kj}}\overline{\sigma_{kj}(\tau)}\frac{\partial}{\partial t}K_2(\tau, t)\,\mathrm{d}\bar{\tau}\right]$$
$$= 2\pi\mathrm{i}\left[\frac{a_{2k}}{2}\sigma(t) + \sigma^{\infty}(t)\right] \tag{3}$$

where $t \in \cup_{j=1}^{N}(L_{1j} \cup L_{2j})$, $k = 1, 2$,

$$\left.\begin{array}{l} a_{2k} = a_{2kj} \\ \sigma(t) = \sigma_{kj}(t) \end{array}\right\} \quad \text{if } t \in L_{kj} \tag{4}$$

$$a_{11j} = \frac{1}{2\mu_{1j}} - \frac{1}{2\mu_{2j}}; \quad a_{21j} = \frac{1 + \kappa_{1j}}{2\mu_{1j}} + \frac{1 + \kappa_{2j}}{2\mu_{2j}}; \quad a_{31j} = \frac{1 + \kappa_{1j}}{2\mu_{1j}} - \frac{1 + \kappa_{2j}}{2\mu_{2j}}; \quad a_{12j} = \frac{1}{2\mu_{2j}} - \frac{1}{2\mu};$$
$$a_{22j} = \frac{1 + \kappa_{2j}}{2\mu_{2j}} + \frac{1 + \kappa}{2\mu}; \quad a_{32j} = \frac{1 + \kappa_{2j}}{2\mu_{2j}} - \frac{1 + \kappa}{2\mu} \tag{5}$$

$$\sigma^{\infty}(t) = -\frac{\kappa + 1}{4\mu}\left[\sigma_{xx}^{\infty} + \sigma_{yy}^{\infty} + \frac{\mathrm{d}\bar{t}}{\mathrm{d}t}(\sigma_{yy}^{\infty} - \sigma_{xx}^{\infty} - 2\mathrm{i}\sigma_{xy}^{\infty})\right] \tag{6}$$

σ_{xx}^{∞}, σ_{yy}^{∞}, and σ_{xy}^{∞} are the stresses at infinity; $\kappa = 3 - 4\nu$ for plane strain; $\kappa = (3 - \nu)/(1 + \nu)$ for plane stress; a bar over a symbol denotes complex conjugation; $\mathrm{d}\bar{t}/\mathrm{d}t = \exp(-2\mathrm{i}\gamma)$ where γ is the angle between the axis Ox and the tangent at point t; and

$$K_1(\tau, t) = \ln\frac{\tau - t}{\bar{\tau} - \bar{t}}; \quad K_2(\tau, t) = \frac{\tau - t}{\bar{\tau} - \bar{t}}$$

The components of the stress tensor σ_{xx}, σ_{yy}, and σ_{xy} and the displacements $u(z) = u_x(z) + \mathrm{i}u_y(z)$ at any point z inside the inclusions and matrix can be calculated from two complex functions $\varphi(z)$ and $\psi(z)$ by using the Kolosov–Muskhelishvili formulae (Muskhelishvili, 1959)

$$\begin{aligned} &2\mu u(z) = \kappa\varphi(z) - z\overline{\varphi'(z)} - \overline{\psi(z)} \\ &\sigma_{xx} + \sigma_{yy} = 4\mathrm{Re}\varphi'(z) \\ &\sigma_{yy} - \sigma_{xx} + 2\mathrm{i}\sigma_{xy} = 2\left[\bar{z}\varphi''(z) + \psi'(z)\right] \end{aligned} \tag{7}$$

The Kolosov–Muskhelishvili potentials can be expressed in terms of integrals of the boundary tractions as follows (Mogilevskaya and Crouch, 2001)

$$\begin{aligned}\varphi(z) &= -\frac{\mu_\ell}{\pi \mathrm{i}(\kappa_\ell+1)}\sum_{j=1}^{N}\sum_{k=1}^{2} a_{1kj}\int_{L_{kj}}\sigma_{kj}(\tau)\ln(\tau-z)\,\mathrm{d}\tau+\varphi^\infty(z)\\ \psi(z) &= -\frac{\mu_\ell}{\pi \mathrm{i}(\kappa_\ell+1)}\sum_{j=1}^{N}\sum_{k=1}^{2}\left[a_{1kj}\int_{L_{kj}}\sigma_{kj}(\tau)\frac{\bar\tau\,\mathrm{d}\tau}{\tau-z}+(a_{3kj}-a_{1kj})\int_{L_{kj}}\overline{\sigma_{kj}(\tau)}\ln(\tau-z)\,\mathrm{d}\bar\tau\right]+\psi^\infty(z)\end{aligned} \tag{8}$$

where μ_ℓ and κ_ℓ are the elastic constants of the ℓth inclusion if $|z-z_\ell|\leqslant R_{1\ell}$, the ℓth interphase if $R_{1\ell}<|z-z_\ell|\leqslant R_{2\ell}$, or else $\mu_\ell=\mu$, $\kappa_\ell=\kappa$ if z is a point of the matrix, and

$$\begin{aligned}\varphi^\infty(z) &= \frac{\mu_\ell(\kappa+1)}{\mu(\kappa_\ell+1)}\,\frac{\sigma_{xx}^\infty+\sigma_{yy}^\infty}{4}z\\ \psi^\infty(z) &= \frac{\mu_\ell(\kappa+1)}{\mu(\kappa_\ell+1)}\,\frac{\sigma_{yy}^\infty-\sigma_{xx}^\infty+2\mathrm{i}\sigma_{xy}^\infty}{2}z\end{aligned} \tag{9}$$

In writing (8) we have neglected constant terms in each expression. It is clear from (7) that these terms would only affect the expressions for the displacements. The missing constants in expressions (8) can, if desired, be found from the conditions of the continuity of the displacements across each boundary L_{kj}.

4. Numerical solution

In order to solve (3), we represent the unknown tractions $\sigma_{kj}(\tau)$ at each boundary L_{kj} by a truncated complex Fourier series of the form

$$\sigma_{kj}(\tau)\approx\sum_{m=1}^{M_j}B_{-mkj}F_{mkj}+\sum_{m=0}^{M_j}B_{mkj}/F_{mkj},\qquad \tau\in L_{kj} \tag{10}$$

where

$$F_{mkj}(\tau)=\left(\frac{R_{kj}}{\tau-z_j}\right)^m \tag{11}$$

It will be seen from the subsequent derivations that the number of terms in the truncated Fourier series must be the same for L_{1j} and L_{2j}. We note, however, that this number need not be the same for all the individual inclusions.

By substituting the expression (10) into equilibrium conditions (1) and (2), we find that

$$B_{-1kj}=0;\quad B_{0kj}\ \text{are real} \tag{12}$$

for all $j=1,\dots,N$ and $k=1,2$.

The complex coefficients B_{-mkj} $(m=1,\dots,M_j)$ and B_{mkj} $(m=0,\dots,M_j)$ in series (10) need to be determined.

All integrals involved in (3) can be evaluated analytically similarly to the case of perfectly bonded inclusions (Mogilevskaya and Crouch, 2001). By substituting the corresponding expressions for those integrals into Eq. (3) we obtain the following system of equations:

(i) $t \in L_{1\ell}$

$$-\frac{c_{11\ell}}{2}\sum_{m=2}^{M_\ell} B_{-m1\ell}F_{m1\ell}(t) + \frac{c_{21\ell}}{2}B_{01\ell} + \frac{c_{31\ell}}{2}\sum_{m=1}^{M_\ell} B_{m1\ell}/F_{m1\ell}(t) - (a_{12\ell}-a_{32\ell})\sum_{m=2}^{M_\ell} B_{-m2\ell}\left(\frac{R_{1\ell}}{R_{2\ell}}\right)^{m-2}F_{m1\ell}(t)$$

$$+ 2a_{12\ell}B_{02\ell} + a_{12\ell}\sum_{m=1}^{M_\ell} B_{m2\ell}/F_{m2\ell}(t) - a_{12\ell}\sum_{m=1}^{M_\ell}(m-1)\overline{B}_{m2\ell}\left(\frac{R_{1\ell}}{R_{2\ell}}\right)^{m}\left(1-\frac{R_{2\ell}^2}{R_{1\ell}^2}\right)F_{m1\ell}(t) + \sum_{k=1}^{2}\sum_{\substack{j=1\\ j\neq\ell}}^{N}\Xi_{1kj}(t)$$

$$= -\frac{\kappa+1}{4\mu}\left[\sigma_{xx}^{\infty} + \sigma_{yy}^{\infty} - F_{21\ell}(t)(\sigma_{yy}^{\infty} - \sigma_{xx}^{\infty} - 2\mathrm{i}\sigma_{xy}^{\infty})\right]$$

(ii) $t \in L_{2\ell}$

$$-\frac{c_{12\ell}}{2}\sum_{m=2}^{M_\ell} B_{-m2\ell}F_{m2\ell}(t) + \frac{c_{22\ell}}{2}B_{02\ell} + \frac{c_{32\ell}}{2}\sum_{m=1}^{M_\ell} B_{m2\ell}/F_{m2\ell}(t) - a_{11\ell}\sum_{m=2}^{M_\ell} B_{-m1\ell}F_{m1\ell}(t)$$

$$+ (2a_{11\ell}-a_{31\ell})B_{01\ell}\left(\frac{R_{1\ell}}{R_{2\ell}}\right)^{2} + (a_{11\ell}-a_{31\ell})\sum_{m=1}^{M_\ell} B_{m1\ell}\left(\frac{R_{1\ell}}{R_{2\ell}}\right)^{m+2}\Big/F_{m2\ell}(t)$$

$$- a_{11\ell}\sum_{m=2}^{M_\ell}(m+1)\overline{B}_{-m1\ell}\left(\frac{R_{1\ell}}{R_{2\ell}}\right)^{m}\left(1-\frac{R_{1\ell}^2}{R_{2\ell}^2}\right)\Big/F_{m2\ell}(t) + \sum_{k=1}^{2}\sum_{\substack{j=1\\ j\neq\ell}}^{N}\Xi_{2kj}(t)$$

$$= -\frac{\kappa+1}{4\mu}\left[\sigma_{xx}^{\infty} + \sigma_{yy}^{\infty} - F_{22\ell}(t)(\sigma_{yy}^{\infty} - \sigma_{xx}^{\infty} - 2\mathrm{i}\sigma_{xy}^{\infty})\right] \tag{13}$$

where

$$c_{1k\ell} = 2a_{1k\ell} + a_{2k\ell} - a_{3k\ell}; \quad c_{2k\ell} = 4a_{1k\ell} - a_{2k\ell} - a_{3k\ell}; \quad c_{3k\ell} = 2a_{1k\ell} - a_{2k\ell} - a_{3k\ell}$$

and

$$\Xi_{pkj}(t) = \Bigg\{ -a_{1kj}\sum_{m=2}^{M_j} B_{-mkj}F_{mkj}(t) + (2a_{1kj}-a_{3kj})B_{0kj}F_{2p\ell}(t)\overline{F_{2kj}(t)} + (a_{1kj}-a_{3kj})\sum_{m=1}^{M_j} B_{mkj}\overline{F_{(m+2)kj}(t)}F_{2p\ell}(t)$$
$$+ a_{1kj}\sum_{m=2}^{M_j}\overline{B}_{-mkj}\left[-1 + (m+1)F_{2p\ell}(t)\overline{F_{2kj}(t)} - mF_{2p\ell}(t)\frac{t-z_j}{\overline{t}-\overline{z_j}}\right]\overline{F_{mkj}(t)}\Bigg\}$$

By writing this equation for all the inclusions, $\ell = 1$ to N, one gets a system of $2N$ complex algebraic equations involving $2\sum_{\ell=1}^{N}(2M_{1\ell}-1)$ complex coefficients $B_{-mk\ell}$ ($m = 2,\ldots,M_\ell,\ k = 1,\ 2$) and $B_{mk\ell}$ ($m = 1,\ldots,M_\ell$, $k = 1$, 2), and $2N$ real coefficients $B_{0k\ell}$.

5. One inclusion

In the particular case of a single inclusion with the center z_ℓ, Eq. (13) can be solved analytically because both sides of this equation represent a truncated complex Fourier series. The two sides of the equation are equal if and only if the corresponding complex coefficients for terms of the same power are equal. As a result we get the following system of equations:

(i) $t \in L_{1\ell}$

$$\begin{aligned}
&-\frac{c_{11\ell}}{2}B_{-m1\ell} - (a_{12\ell} - a_{32\ell})\left(\frac{R_{1\ell}}{R_{2\ell}}\right)^{m-2} B_{-m2\ell} + (m-1)a_{12\ell}\overline{B}_{m2\ell}\left(\frac{R_{1\ell}}{R_{2\ell}}\right)^{m-2}\left(1 - \frac{R_{1\ell}^2}{R_{2\ell}^2}\right) \\
&= \begin{cases} \frac{\kappa+1}{4\mu}(\sigma_{yy}^\infty - \sigma_{xx}^\infty - 2\mathrm{i}\sigma_{xy}^\infty), & m = 2 \\ 0, & m > 2 \end{cases} \\
&\frac{c_{21\ell}}{2}B_{01\ell} + 2a_{12\ell}B_{02\ell} = -\frac{\kappa+1}{4\mu}\left(\sigma_{xx}^\infty + \sigma_{yy}^\infty\right) \\
&\frac{c_{31\ell}}{2}B_{m1\ell} + a_{12\ell}\left(\frac{R_{1\ell}}{R_{2\ell}}\right)^m B_{m2\ell} = 0, \quad m > 0
\end{aligned} \tag{14}$$

(ii) $t \in L_{2\ell}$

$$\begin{aligned}
&-\frac{c_{12\ell}}{2}B_{-m2\ell} - a_{11\ell}\left(\frac{R_{1\ell}}{R_{2\ell}}\right)^m B_{-m1\ell} = \begin{cases} \frac{\kappa+1}{4\mu}(\sigma_{yy}^\infty - \sigma_{xx}^\infty - 2\mathrm{i}\sigma_{xy}^\infty), & m = 2 \\ 0, & m > 2 \end{cases} \\
&\frac{c_{22\ell}}{2}B_{02\ell} + (2a_{11\ell} - a_{31\ell})\left(\frac{R_{1\ell}}{R_{2\ell}}\right)^2 B_{01\ell} = -\frac{\kappa+1}{4\mu}\left(\sigma_{xx}^\infty + \sigma_{yy}^\infty\right) \\
&\frac{c_{32\ell}}{2}B_{m2\ell} + (a_{11\ell} - a_{31\ell})\left(\frac{R_{1\ell}}{R_{2\ell}}\right)^{m+2} B_{m1\ell} + a_{11\ell}(m+1)\left(\frac{R_{1\ell}}{R_{2\ell}}\right)^m \left[\left(\frac{R_{1\ell}}{R_{2\ell}}\right)^2 - 1\right]\overline{B}_{-m1\ell} = 0, \quad m > 0
\end{aligned} \tag{15}$$

We see from expressions (14) and (15) that the coefficients $B_{-m1\ell}$, $B_{-m2\ell}$ and $B_{m1\ell}$, $B_{m2\ell}$ are involved in the same equations of the system. This means that number of terms in the truncated Fourier series must be the same for L_{1j} and L_{2j}. The solution of system (14) and (15) leads to the following expressions for the only nonzero coefficients $B_{-21\ell}$, $B_{01\ell}$, $B_{21\ell}$, and $B_{-22\ell}$, $B_{02\ell}$, $B_{22\ell}$:

$$\begin{aligned}
B_{-21\ell} &= \frac{-(\kappa+1)(\sigma_{yy}^\infty - \sigma_{xx}^\infty - 2\mathrm{i}\sigma_{xy}^\infty)(a_{22\ell} + a_{32\ell})}{8\mu\Lambda} \\
B_{01\ell} &= \frac{(\kappa+1)\left(\sigma_{xx}^\infty + \sigma_{yy}^\infty\right)(a_{22\ell} + a_{32\ell})}{2\mu[c_{21\ell}c_{22\ell} - 8a_{12\ell}(2a_{11\ell} - a_{31\ell})R_{1\ell}^2/R_{2\ell}^2]} \\
B_{21\ell} &= -3a_{11\ell}a_{12\ell}\left(\frac{R_{1\ell}}{R_{2\ell}}\right)^2\left[\left(\frac{R_{1\ell}}{R_{2\ell}}\right)^2 - 1\right]\overline{B}_{-21\ell}\Big/\Lambda \\
B_{-22\ell} &= -2\left[\frac{(\kappa+1)(\sigma_{yy}^\infty - \sigma_{xx}^\infty - 2\mathrm{i}\sigma_{xy}^\infty)}{4\mu} + a_{11\ell}\left(\frac{R_{1\ell}}{R_{2\ell}}\right)^2 B_{-21\ell}\right]\Big/c_{12\ell} \\
B_{02\ell} &= -\frac{(\kappa+1)\left(\sigma_{xx}^\infty + \sigma_{yy}^\infty\right)\left[c_{21\ell} - 2(2a_{11\ell} - a_{31\ell})R_{1\ell}^2/R_{2\ell}^2\right]}{2\mu[c_{21\ell}c_{22\ell} - 8a_{12\ell}(2a_{11\ell} - a_{31\ell})R_{1\ell}^2/R_{2\ell}^2]} \\
B_{22\ell} &= -\frac{c_{31\ell}}{2a_{12\ell}}\left(\frac{R_{2\ell}}{R_{1\ell}}\right)^2 B_{21\ell}
\end{aligned} \tag{16}$$

where

$$\Lambda = a_{12\ell}(a_{11\ell} - a_{31\ell})\left(\frac{R_{1\ell}}{R_{2\ell}}\right)^4 - \left(\frac{R_{2\ell}}{R_{1\ell}}\right)^2\frac{c_{31\ell}c_{32\ell}}{4}$$

$$\Delta = \frac{c_{12\ell}}{4}\left\{c_{11\ell} + 3c_{31\ell}a_{11\ell}a_{12\ell}\left[\left(\frac{R_{1\ell}}{R_{2\ell}}\right)^2 - 1\right]^2\Big/\Lambda\right\} - a_{11\ell}(a_{12\ell} - a_{32\ell})\left(\frac{R_{1\ell}}{R_{2\ell}}\right)^2$$

Apart from notation this result agrees with the solution obtained by Ru (1999).

For future reference it is useful to rewrite a real analog of (14) and (15) in matrix form. We introduce the vector of the unknowns as follows

$$\mathbf{X}_\ell = \begin{bmatrix}\mathbf{X}_{1\ell}\\ \mathbf{X}_{2\ell}\end{bmatrix} \tag{17}$$

where the subvector $\mathbf{X}_{k\ell}$, $k = 1$ or 2, is defined as

$$\mathbf{X}^{\mathrm{T}}_{k\ell} = \left\{\mathrm{Re}B_{-M_\ell k\ell}, \mathrm{Im}B_{-M_\ell k\ell}, \ldots, \mathrm{Re}B_{-2k\ell}, \mathrm{Im}B_{-2k\ell}, B_{0k\ell}, \mathrm{Re}B_{1k\ell}, \mathrm{Im}B_{1k\ell}, \ldots, \mathrm{Re}B_{M_\ell k\ell}, \mathrm{Im}B_{M_\ell k\ell}\right\} \tag{18}$$

A real analog of the system (14) and (15) can then be written in matrix form as

$$\mathbf{A}_{\ell\ell}\mathbf{X}_\ell = \mathbf{D}_\ell \tag{19}$$

where the vector of the right-hand side $\mathbf{D}_\ell$ has the form

$$\mathbf{D}_\ell = \begin{bmatrix}\mathbf{D}_0\\ \mathbf{D}_0\end{bmatrix} \tag{20}$$

in which the subvector $\mathbf{D}_0$ is the same as for an isolated perfectly bonded inclusion (expression (30) from Mogilevskaya and Crouch, 2001).

The square matrix $\mathbf{A}_{\ell\ell}$ of dimension $(n_\ell \times n_\ell)$ with

$$n_\ell = 2(4M_\ell - 1) \tag{21}$$

in (19) can be written as

$$\mathbf{A}_{\ell\ell} = \begin{bmatrix}\mathbf{A}_{11}(\ell) & \mathbf{A}_{12}(\ell)\\ \mathbf{A}_{21}(\ell) & \mathbf{A}_{22}(\ell)\end{bmatrix} \tag{22}$$

where four square submatrices $\mathbf{A}_{11}(\ell)$, $\mathbf{A}_{12}(\ell)$, $\mathbf{A}_{21}(\ell)$, and $\mathbf{A}_{22}(\ell)$ have the dimension $4M_\ell - 1 \times 4M_\ell - 1$. The diagonal submatrices $\mathbf{A}_{11}(\ell)$ and $\mathbf{A}_{22}(\ell)$ correspond to the cases of isolated perfectly bonded inclusions (expression (32) from Mogilevskaya and Crouch, 2001): one with the radius $R_{1\ell}$ and the elastic properties of the ℓth inclusion, and the other with radius $R_{2\ell}$ and elastic properties of the ℓth interphase. The submatrices $\mathbf{A}_{12}(\ell)$ and $\mathbf{A}_{21}(\ell)$ are triangular and sparse. Taking into account that the matrix $\mathbf{A}_{\ell\ell}$ is sparse, a special Gauss-elimination type procedure can be designed to invert $\mathbf{A}_{\ell\ell}$ with modest computational cost.

6. *N* inclusions

In the general case of N inclusions we use the Galerkin method (e.g. Brebbia et al., 1984) to get a linear algebraic system. For the case when $t \in L_{1\ell}$ $(L_{2\ell})$ we successively multiply both sides of Eq. (13) by the powers $(t - z_\ell)^p$ $[p = -(M_\ell + 1), -M_\ell, \ldots, -1, 1, 2, \ldots, M_\ell - 1]$ and integrate over $L_{1\ell}$ $(L_{2\ell})$. The integrations can again be done analytically similarly as in Mogilevskaya and Crouch (2001). This gives the following systems of $4M_\ell$ equations with respect to the unknown coefficients:

(i) $M_\ell - 1$ equations ($p = 1, \ldots, M_\ell - 1$)

$$-\frac{c_{11\ell}}{2}B_{-(p+1)1\ell} - (a_{12\ell} - a_{32\ell})\left(\frac{R_{1\ell}}{R_{2\ell}}\right)^{p-1}B_{-(p+1)2\ell} - pa_{12\ell}\left[\left(\frac{R_{1\ell}}{R_{2\ell}}\right)^2 - 1\right]\left(\frac{R_{1\ell}}{R_{2\ell}}\right)^{p-1}\overline{B}_{(p+1)2\ell}$$
$$+ \sum_{\substack{j=1\\j\neq\ell}}^{N}\overline{F_{(p-1)1\ell}(z_j)}\sum_{k=1}^{2}\left\{(2a_{1kj} - a_{3kj})p\overline{F_{2kj}(z_\ell)}B_{0kj} + a_{1kj}\sum_{m=2}^{M_j}p\binom{m+p-1}{m-1}\overline{B}_{-mkj}\overline{F_{mkj}(z_\ell)}\right.$$
$$\left.\times\left[\left(\overline{F_{21\ell}(z_j)}\frac{m+p}{p+1} + \overline{F_{2kj}(z_\ell)}\frac{m+p}{m} - \frac{z_\ell - z_j}{\overline{z_\ell} - \overline{z_j}}\right)\right] + (a_{1kj} - a_{3kj})\sum_{m=1}^{M_j}\binom{m+p}{m+1}B_{mkj}\overline{F_{(m+2)kj}(z_\ell)}\right\}$$
$$= \begin{cases} \frac{\kappa+1}{4\mu}(\sigma_{yy}^\infty - \sigma_{xx}^\infty - 2\mathrm{i}\sigma_{xy}^\infty), & p = 1\\ 0, & p \neq 1\end{cases} \tag{23}$$

(ii) the equation

$$\frac{c_{21\ell}}{2}B_{01\ell} + 2a_{12\ell}B_{02\ell} - \sum_{\substack{j=1\\j\neq\ell}}^{N}\sum_{k=1}^{2}a_{1kj}\sum_{m=2}^{M_j}\left[B_{-mkj}F_{mkj}(z_\ell) + \overline{B}_{-mkj}\overline{F_{mkj}(z_\ell)}\right] = -\frac{\kappa+1}{4\mu}(\sigma_{xx}^\infty + \sigma_{yy}^\infty) \tag{24}$$

(iii) M_ℓ equations ($p = 2, \ldots, M_\ell + 1$)

$$\frac{c_{31\ell}}{2}B_{(p-1)1\ell} + a_{12\ell}B_{(p-1)2\ell}\left(\frac{R_{1\ell}}{R_{2\ell}}\right)^{p-1} - \sum_{\substack{j=1\\j\neq\ell}}^{N}F_{(p-1)1\ell}(z_j)\sum_{k=1}^{2}a_{1kj}\sum_{m=2}^{M_j}\binom{m+p-2}{m-1}B_{-mkj}F_{mkj}(z_\ell) = 0 \tag{25}$$

(iv) $M_\ell - 1$ equations ($p = 1, \ldots, M_\ell - 1$)

$$-\frac{c_{12\ell}}{2}B_{-(p+1)2\ell} - a_{11\ell}\left(\frac{R_{1\ell}}{R_{2\ell}}\right)^{p+1}B_{-(p+1)1\ell} + \sum_{\substack{j=1\\j\neq\ell}}^{N}\overline{F_{(p-1)2\ell}(z_j)}\sum_{k=1}^{2}\left\{(2a_{1kj} - a_{3kj})p\overline{F_{2kj}(z_\ell)}B_{0kj}\right.$$
$$+ a_{1kj}\sum_{m=2}^{M_j}p\binom{m+p-1}{m-1}\overline{B}_{-mkj}\overline{F_{mkj}(z_\ell)}\left[\left(\overline{F_{22\ell}(z_j)}\frac{m+p}{p+1} + \overline{F_{2kj}(z_\ell)}\frac{m+p}{m} - \frac{z_\ell - z_j}{\overline{z_\ell} - \overline{z_j}}\right)\right]$$
$$\left.+ (a_{1kj} - a_{3kj})\sum_{m=1}^{M_j}\binom{m+p}{m+1}B_{mkj}\overline{F_{(m+2)kj}(z_\ell)}\right\} = \begin{cases} \frac{\kappa+1}{4\mu}(\sigma_{yy}^\infty - \sigma_{xx}^\infty - 2\mathrm{i}\sigma_{xy}^\infty), & p = 1\\ 0, & p \neq 1\end{cases} \tag{26}$$

(v) the equation

$$\frac{c_{22\ell}}{2}B_{02\ell} + (2a_{11\ell} - a_{31\ell})B_{01\ell}\left(\frac{R_{1\ell}}{R_{2\ell}}\right)^2 - \sum_{\substack{j=1\\j\neq\ell}}^{N}\sum_{k=1}^{2}a_{1kj}\sum_{m=2}^{M_j}\left[B_{-mkj}F_{mkj}(z_\ell) + \overline{B}_{-mkj}\overline{F_{mkj}(z_\ell)}\right]$$
$$= -\frac{\kappa+1}{4\mu}\left(\sigma_{xx}^\infty + \sigma_{yy}^\infty\right) \tag{27}$$

(vi) M_ℓ equations ($p = 2, \ldots, M_\ell + 1$)

$$\frac{c_{32\ell}}{2} B_{(p-1)2\ell} + (a_{11\ell} - a_{31\ell}) B_{(p-1)1\ell} \left(\frac{R_{1\ell}}{R_{2\ell}}\right)^{p+1} + p a_{11\ell} \left(\frac{R_{1\ell}}{R_{2\ell}}\right)^{p-1} \left[\left(\frac{R_{1\ell}}{R_{2\ell}}\right)^{2} - 1\right] \overline{B}_{-(p-1)1\ell}$$

$$- \sum_{\substack{j=1 \\ j \neq \ell}}^{N} F_{(p-1)2\ell}(z_j) \sum_{k=1}^{2} a_{1kj} \sum_{m=2}^{M_j} \binom{m+p-2}{m-1} B_{-mkj} F_{mkj}(z_\ell) = 0 \tag{28}$$

where the binomial coefficients are defined as

$$\binom{n}{m} = \frac{n!}{m!(n-m)!} \tag{29}$$

By writing these equations for $\ell = 1, \ldots, N$ and separating real and imaginary parts, we get finally the real system of $\sum_{\ell=1}^{N} n_\ell$ (where n_ℓ is given by (21)) linear algebraic equations

$$\mathbf{AX} = \mathbf{D} \tag{30}$$

The matrix of this system has the following form

$$\mathbf{A} = \begin{bmatrix} \mathbf{A}_{11} & \cdots & \mathbf{A}_{1N} \\ \vdots & \vdots & \vdots \\ \mathbf{A}_{N1} & \cdots & \mathbf{A}_{NN} \end{bmatrix} \tag{31}$$

where $\mathbf{A}_{\ell\ell}$ is submatrix (22). The submatrix $\mathbf{A}_{\ell j}$ ($j \neq \ell$) of dimension ($n_\ell \times n_j$) is a full submatrix that expresses the influence of the jth inclusion on the ℓth inclusion. The vector of unknowns $\mathbf{X}$ and the right-hand side vector $\mathbf{D}$ can be written as

$$\mathbf{X} = \begin{bmatrix} \mathbf{X}_1 \\ \vdots \\ \mathbf{X}_N \end{bmatrix}; \quad \mathbf{D} = \begin{bmatrix} \mathbf{D}_1 \\ \vdots \\ \mathbf{D}_N \end{bmatrix} \tag{32}$$

where subvectors $\mathbf{X}_\ell$ and $\mathbf{D}_\ell$ are given by (17) and (20).

The system (30) can be solved by using a Gauss–Seidel iterative algorithm (Golub and Van Loan, 1996). The number of terms M_ℓ of the complex Fourier series can be determined during the external iterative procedure in the same manner as described in Mogilevskaya and Crouch (2001).

7. Calculation of the displacements, stresses, and strains

The Kolosov–Muskhelishvili potentials $\varphi(z)$ and $\psi(z)$ can be obtained by substituting (10) into (8). Again, all the integrals can all be calculated analytically. Letting

$$\begin{aligned} \Omega_{1kj}(z) &= a_{1kj} R_{kj} \sum_{m=2}^{M_j} B_{-mkj} F_{(m-1)kj}(z)/(m-1) \\ \Omega_{2kj}(z) &= a_{1kj} \left[\left(R_{kj} F_{1kj}(z) + \bar{z}_j\right)\right] \sum_{m=2}^{M_j} B_{-mkj} F_{mkj}(z) + (2a_{1kj} - a_{3kj}) B_{0kj} R_{kj} F_{1kj}(z) \\ &\quad + (a_{1kj} - a_{3kj}) R_{kj} \sum_{m=1}^{M_j} \overline{B}_{mkj} F_{(m+1)kj}(z)/(m+1) \end{aligned} \tag{33}$$

and neglecting constant terms, the final expressions for the potentials can be written as follows:

(i) the evaluation point is inside an inclusion (e.g. $|z - z_\ell| \leqslant R_{1\ell}$)

$$\varphi(z) = \frac{2\mu_{1\ell}}{\kappa_{1\ell}+1} \sum_{k=1}^{2} \left\{ a_{1k\ell} R_{k\ell} \sum_{m=0}^{M_\ell} B_{mk\ell} / \left[(m+1) F_{(m+1)k\ell}(z) \right] + \sum_{\substack{j=1 \\ j \neq \ell}}^{N} \Omega_{1kj}(z) \right\} + \varphi^\infty(z)$$

$$\psi(z) = -\frac{2\mu_{1\ell}}{\kappa_{1\ell}+1} \sum_{k=1}^{2} \left\{ a_{1k\ell} [R_{k\ell} F_{1k\ell}(z) + \overline{z_\ell}] \sum_{m=1}^{M_\ell} B_{mk\ell} / F_{mk\ell}(z) \right. \quad (34)$$

$$\left. + (a_{3k\ell} - a_{1k\ell}) R_{k\ell} \sum_{m=2}^{M_\ell} \overline{B}_{-mk\ell} / \left[(m-1) F_{(m-1)k\ell}(z) \right] - \sum_{\substack{j=1 \\ j \neq \ell}}^{N} \Omega_{2kj}(z) \right\} + \psi^\infty(z)$$

(ii) the evaluation point is inside an interphase (e.g. $R_{1\ell} < |z - z_\ell| \leqslant R_{2\ell}$)

$$\varphi(z) = \frac{2\mu_{2\ell}}{\kappa_{2\ell}+1} \left\{ a_{11\ell} R_{1\ell} \sum_{m=2}^{M_\ell} B_{-m1\ell} F_{(m-1)1\ell}(z)/(m-1) \right.$$

$$\left. + a_{12\ell} R_{2\ell} \sum_{m=0}^{M_\ell} B_{m2\ell} / \left[(m+1) F_{(m+1)2\ell}(z) \right] + \sum_{\substack{j=1 \\ j \neq \ell}}^{N} \sum_{k=1}^{2} \Omega_{1kj}(z) \right\} + \varphi^\infty(z)$$

$$\psi(z) = \frac{2\mu_{2\ell}}{\kappa_{2\ell}+1} \left\{ (2a_{11\ell} - a_{31\ell}) B_{01\ell} R_{1\ell} F_{11\ell}(z) + a_{11\ell} [R_{1\ell} F_{11\ell}(z) + \overline{z_\ell}] \sum_{m=2}^{M_\ell} B_{-m1\ell} F_{m1\ell}(z) \right. \quad (35)$$

$$- a_{12\ell} [R_{2\ell} F_{12\ell}(z) + \overline{z_\ell}] \sum_{m=1}^{M_\ell} B_{m2\ell} / F_{m2\ell}(z) + (a_{11\ell} - a_{31\ell}) R_{1\ell} \sum_{m=1}^{M_\ell} \overline{B}_{m1\ell} F_{(m+1)1\ell}(z)/(m+1)$$

$$\left. + (a_{12\ell} - a_{32\ell}) R_{2\ell} \sum_{m=2}^{M_\ell} \overline{B}_{-m2\ell} / \left[(m-1) F_{(m-1)2\ell}(z) \right] + \sum_{\substack{j=1 \\ j \neq \ell}}^{N} \sum_{k=1}^{2} \Omega_{2kj}(z) \right\} + \psi^\infty(z)$$

(iii) the evaluation point z is inside the matrix

$$\varphi(z) = \frac{2\mu}{\kappa+1} \sum_{j=1}^{N} \sum_{k=1}^{2} \Omega_{1kj}(z) + \varphi^\infty(z)$$

$$\psi(z) = \frac{2\mu}{\kappa+1} \sum_{j=1}^{N} \sum_{k=1}^{2} \Omega_{2kj}(z) + \psi^\infty(z) \quad (36)$$

The displacements and stresses inside the inclusions, interphases, and the matrix can be calculated by using formulae (7), (34)–(36), and (9). The complete expressions are given in Appendixes A and B.

The strains inside the inclusions, interphases, and the matrix can be found from the following relations

$$\begin{aligned} \epsilon_{xx} + \varepsilon_{yy} &= \frac{1-2\nu_\ell}{2\mu_\ell}(\sigma_{xx}+\sigma_{yy}) \\ \varepsilon_{yy} - \epsilon_{xx} + 2\mathrm{i}\epsilon_{xy} &= \frac{1}{2\mu_\ell}(\sigma_{yy}-\sigma_{xx}+2\mathrm{i}\sigma_{xy}) \end{aligned} \tag{37}$$

where ν_ℓ and μ_ℓ are defined as at the end of Section 3.

8. Numerical examples

8.1. Single inclusion

We showed in Section 5 that our approach gives the analytical solution for the case of a single inclusion. Nevertheless, we perform numerical simulations for this simple case to study two different interphase regimes described by Benveniste and Miloh (2001): a spring type interphase and a membrane type interphase.

Consider a circular inclusion of unit radius ($R = 1$) centered at $z = 0$ and let the thickness of the interphase be h. Benveniste and Miloh (2001) represented a thin interphase by a curve separating the fiber and the matrix, and, depending on the interphase properties, showed that seven distinct regimes exist when the parameter $\epsilon = h/L \ll 1$ (L is a typical radius of curvature for the curve representing the interphase). We assume that ϵ (in our case $\epsilon = h/R = h$) is equal to 10^{-3}. We suppose for simplicity that the Poisson's ratios of the fiber, matrix, and interphase are the same: $\nu_{\text{fiber}} = \nu_{\text{matrix}} = \nu_{\text{interphase}} = 0.35$. For the shear moduli we assume that $\mu_{\text{fiber}}/\mu_{\text{matrix}} = 5$. The dimensionless Lamé parameters of the interphase introduced by Benveniste and Miloh (2001) are defined as

$$\left(\tilde{\lambda}_{\text{interphase}}, \tilde{\mu}_{\text{interphase}}\right) = \left(\lambda_{\text{interphase}}, \mu_{\text{interphase}}\right)/(\lambda_0 + 2\mu_0)$$

where

$$\lambda_0 = (\lambda_{\text{fiber}} + \lambda_{\text{matrix}})/2, \quad \mu_0 = (\mu_{\text{fiber}} + \mu_{\text{matrix}})/2$$

8.1.1. Spring type interphase

In this case the tractions are continuous through the interphase and jumps of the normal and shear components of displacement are proportional to the corresponding components of traction, i.e.

$$\Delta u_s = \eta_s \sigma_s, \quad \Delta u_n = \eta_n \sigma_n \tag{38}$$

Benveniste and Miloh (2001) showed using an asymptotic analysis that a spring type interphase exists when the following conditions are satisfied

$$\tilde{\lambda}_{\text{interphase}} \sim \epsilon, \quad \tilde{\mu}_{\text{interphase}} \sim \epsilon \tag{39}$$

Following Hashin (1990, 1991) they express the coefficients η_s and η_n via interphase parameters as follows

$$\eta_s = h/\mu_{\text{interphase}}, \quad \eta_n = h/(\lambda_{\text{interphase}} + 2\mu_{\text{interphase}}) \tag{40}$$

We solve the problem of a single inclusion under uniaxial tension parallel to the x axis using the approach explained in Section 5. To satisfy (39) we take

$$\mu_{\text{interphase}}/\mu_{\text{matrix}} = 13 \times 10^{-3}$$

For comparison with Benveniste and Miloh (2001) we define the jumps in the normal and shear components of displacement and traction as the following differences between their values on the boundary of the interphase L_2 and the boundary of the inclusion L_1 (note that in our analysis the displacements and tractions are continuous throughout the interphase):

$$\Delta\sigma_n = \sigma_n|_{L_2} - \sigma_n|_{L_1}, \quad \Delta\sigma_s = \sigma_s|_{L_2} - \sigma_s|_{L_1}, \quad \Delta u_n = u_n|_{L_2} - u_n|_{L_1}, \quad \Delta u_s = u_s|_{L_2} - u_s|_{L_1} \tag{41}$$

In the problem under consideration we find that zero traction jump conditions are satisfied to within 3 decimal places. Using (40) we also find that $\eta_n = (3R/169)/\mu_{\text{matrix}}$, $\eta_s = (R/13)/\mu_{\text{matrix}}$. Plots of Δu_s, $\eta_s\sigma_s$ and Δu_n, $\eta_n\sigma_n$ are shown in Fig. 2, from which we conclude that the spring type conditions (38) are well satisfied.

Note that if we solve the same single inclusion problem using the approach from Mogilevskaya and Crouch (2002) (i.e. assuming that (a) the thickness of the interphase layer is neglected, (b) tractions are continuous across the interphase, and (c) spring type conditions (38) are enforced along the boundary of the inclusion) we will get results that are within plotting accuracy of ones plotted in Fig. 2.

8.1.2. Discussion of the problem of overlapping

It can be concluded from Fig. 2 that the normal displacement jump Δu_n is negative along some parts of the boundary (i.e. when $70° \leqslant \theta \leqslant 90°$). This means that if the thickness of the interphase is neglected, the fibers and matrix overlap along these parts. This physically unrealistic behavior is considered as the main shortcoming of the spring type interface model. It is therefore of interest to see whether the present model with an interphase layer will eliminate the overlapping.

In the example considered above, Δu_n reaches its minimum at the point $\theta = 90°$ where $\Delta u_n \approx -3.07 \times 10^{-3} = -3.07 \times h$. Thus, overlapping still takes place even if the interphase layer is present.

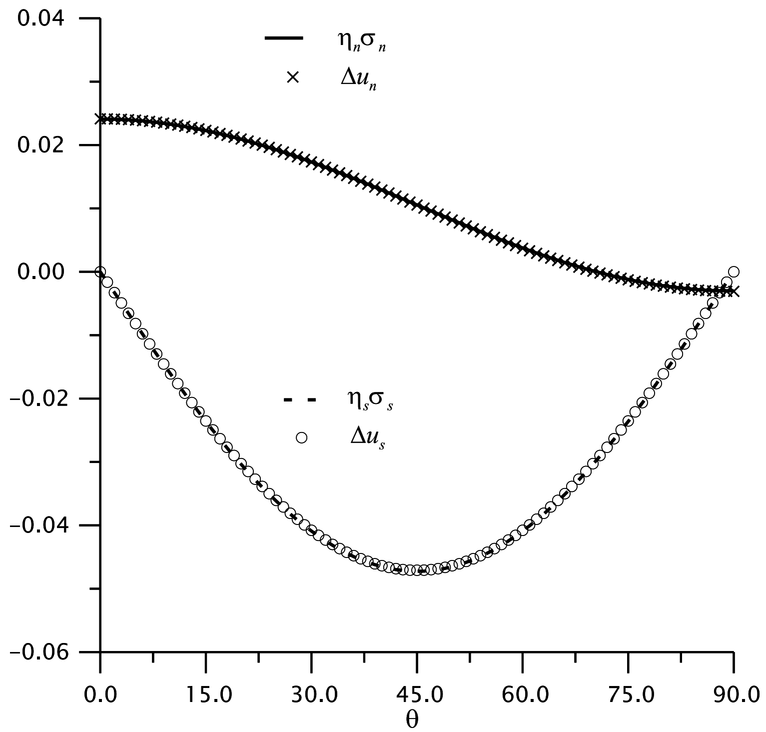

Fig. 2. Spring type interphase.

On the other hand, one could always prevent the overlapping by proportionally increasing the interphase thickness h and shear modulus $\mu_{\text{interphase}}$ by a factor of 3.07 (so that conditions (39) are still satisfied). Another way of preventing overlapping is by proportionally reducing the load. Note that for the spring type interface model (when the thickness of the interphase is neglected) those procedures would not prevent overlapping but just decrease its amplitude.

In conclusion, the problem of overlapping is not completely eliminated by introducing the interphase layer, but the phenomenon can be attributed to rather extreme cases of interphase conditions. It should be noted that for practical problems of coated inclusions these extreme conditions are not likely to occur.

8.1.3. Membrane type interphase

In this case the displacements are continuous through the interphase and jumps of normal and shear components of traction satisfy the following conditions (written here for the particular case of a circular boundary)

$$\Delta\sigma_n = P\varepsilon_{\theta\theta}, \quad \Delta\sigma_s = -P\frac{\partial\varepsilon_{\theta\theta}}{\partial s_0} \tag{42}$$

where $\varepsilon_{\theta\theta}$ is the circumferential strain at the interphase boundary from the interphase side, s_0 is arc length and

$$P = \frac{2\mu_{\text{interphase}}}{1 - \nu_{\text{interphase}}}h$$

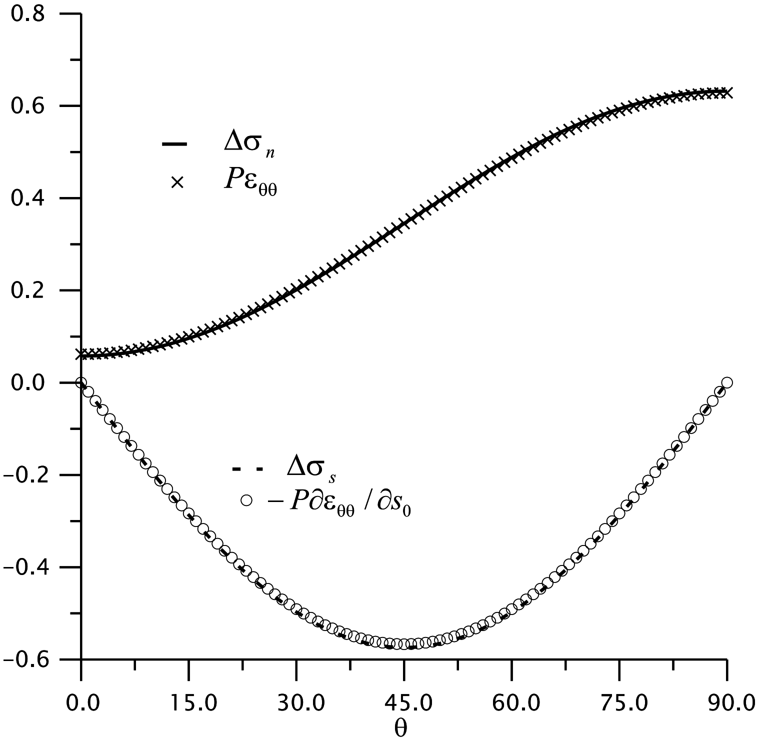

Fig. 3. Membrane type interphase.

According to Benveniste and Miloh (2001), such an interphase exists when

$$\tilde{\lambda}_{\text{interphase}} \sim 1/\epsilon, \quad \tilde{\mu}_{\text{interphase}} \sim 1/\epsilon \tag{43}$$

We again solve the problem of a single inclusion under uniaxial tension along the x axis using the approach explained in Section 5. To satisfy (43) we take

$$\mu_{\text{interphase}}/\mu_{\text{matrix}} = 13 \times 10^3$$

We calculate the jumps in the normal and shear components of displacement and traction using (41), as well as expressions for $P\varepsilon_{\theta\theta}$ and $-P\partial\varepsilon_{\theta\theta}/\partial s_0$. The jumps in the displacements are found to be zero to within 4 decimal places. The results of the comparisons of $P\varepsilon_{\theta\theta}$ and $-P\partial\varepsilon_{\theta\theta}/\partial s_0$ with $\Delta\sigma_n$ and $\Delta\sigma_s$ are shown in Fig. 3, where it can be seen that the membrane type conditions (42) are accurately represented.

8.2. Two inclusions

To study the interaction between inclusions with interphases we consider first a case of two coated copper inclusions inside an infinite epoxy matrix (Fig. 4). The properties of the inclusions and matrix are taken from the paper by Al-Ostaz and Jasiuk (1996), who considered the *plane stress* case. Both inclusions have radius $R = 3.2$ mm and are centered along the x axis. A uniaxial stress $\sigma_{yy} = \sigma_0 = 3.39$ MPa is applied at infinity. In our calculations we assume *plane strain* conditions. The elastic properties of the inclusions, coatings, and matrix (transformed for the plane strain case) are listed in Table 1.

Following Al-Ostaz and Jasiuk (1996) we suppose first that the thicknesses of the interphases are the same for both inclusions (0.8 mm) and the distance between their centers is 11.2 mm. Calculations are performed for the cases of stiff and compliant coatings as well as a reference case of a perfectly bonded inclusion without an interphase (i.e. the elastic properties in the coatings are the same as in the matrix). The accuracy parameters δ_1 and δ_2 used by Mogilevskaya and Crouch (2001) for the Gauss–Seidel and external

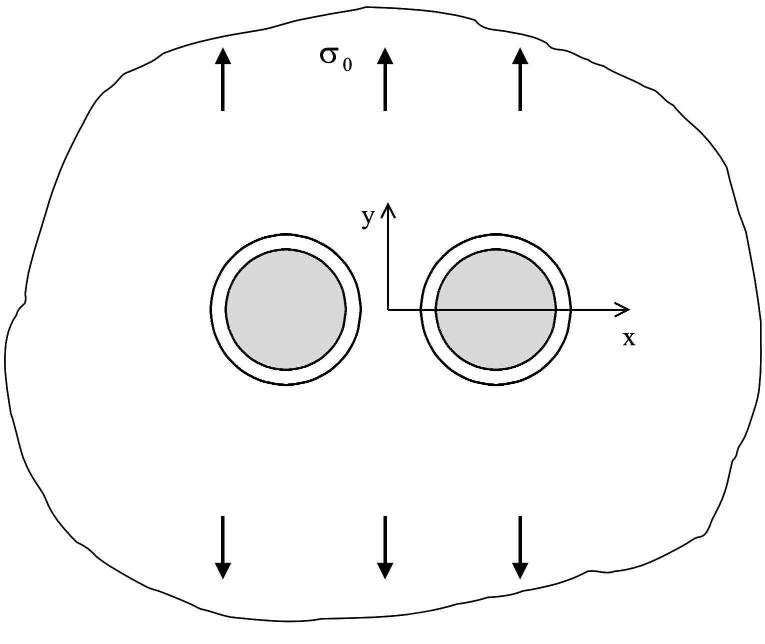

Fig. 4. Two inclusion under uniaxial tension $\sigma_{yy}^{\infty} = \sigma_0$.

Table 1
Elastic properties of the inclusions, coatings and matrix

Material	v	E (MPa)	E/E_{matrix}
Inclusion	0.2537	112220.22	38.9
Matrix	0.2647	2884.63	1
Compliant coating	0.2647	193.27	0.067
Stiff coating	0.2647	57692.64	20.0

iterative algorithms are chosen as 10^{-6} and 10^{-3}, respectively. The number of terms in Fourier series (the same for both inclusions) needed to achieve the chosen accuracy was equal to 9 to for the case of perfect bonding, 6 for the compliant coating, and 9 for the stiff coating.

Al-Ostaz and Jasiuk (1996) presented results for these problems in the form of the maximum normalized effective stress $\sigma_{\text{eff}}/\sigma_0 = [(\sigma_{rr} - \sigma_{\theta\theta})^2 + \sigma_{rr}^2 + \sigma_{\theta\theta}^2 + 6\sigma_{r\theta}^2]^{1/2}/(\sqrt{2}\sigma_0)$ in the matrix, inclusions, and coatings. It is not feasible for us to make a direct comparison with their calculations for two reasons. First, Al-Ostaz and Jasiuk placed the inclusions in a finite plate of dimension $3R \times 5R$ whereas we have used an infinite region. Second and more important, they did not specify the points where the maximum values of $\sigma_{\text{eff}}/\sigma_0$ were calculated. Instead of a direct comparison, we present the distribution of $\sigma_{\text{eff}}/\sigma_0$ along the x axis for the different types of coatings (Fig. 5). Due to symmetry, the results are presented for $x \geqslant 0$.

One can see from Fig. 5 that, compared to the case of a perfect bond, a stiff coating increases the effective stresses inside the inclusion (2.4 mm $\leqslant x \leqslant$ 8.8 mm), except for a small area in its center where a small relaxation zone exists. Effective stresses in the coating (1.6 mm $\leqslant x <$ 2.4 mm and 8.8 mm $< x \leqslant$ 9.6 mm) are much higher than for the perfect bond case; the effective stresses in the matrix are relaxed. For the case

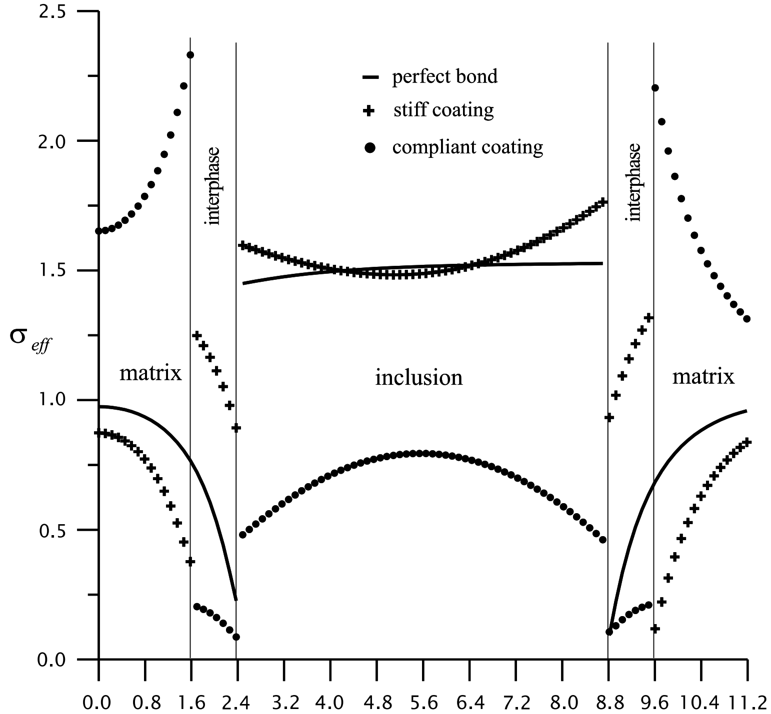

Fig. 5. Distribution of $\sigma_{\text{eff}}/\sigma_0$ along axis Ox.

of a compliant coating the results are reversed: the effective stresses in the inclusion and coating are relaxed, and are concentrated in the matrix near matrix–coating boundary. Qualitatively these results agree with these reported by Al-Ostaz and Jasiuk (1996).

To characterize the global behavior of the stress fields we present contours of the normalized principal stress difference $(\sigma_1 - \sigma_2)/\sigma_0$ (twice the magnitude of the normalized shear stress) for the cases of different coatings (Figs. 6–8). Due to symmetry, the results are presented for $x \geqslant 0$, $y \geqslant 0$. One can see that in the case of a perfect bond the load is mostly carried by the inclusions. A compliant coating releases the stresses inside the inclusions and coatings, and the matrix carries most of the load. A stiff coating increases the stresses in the inclusions and coatings, and the maximum normalized principal stress difference is located near the inclusion–coating boundary.

Fig. 9 shows contours of the normalized principal stress difference $(\sigma_1 - \sigma_2)/\sigma_0$ for the case when inclusions with stiff coatings are near touching (the distance between the centers of the inclusions is equal to 8.2 mm). The number of terms in the Fourier series for this case is equal to 23 for both inclusions (the parameters δ_1 and δ_2 are taken to be the same as above). Fig. 10 illustrates the effect of interactions of the inclusions with the different coatings and interphase thickness. The left and right inclusions have stiff and compliant coatings, respectively. The distance between the centers of the inclusions is equal to 8.2 mm. The thickness of the interphase for the left inclusion is 0.8 mm and for the right one is 0.4 mm. The number of terms in Fourier series for this case is equal to 16 for the left inclusion and 13 for the right one. Due to symmetry, the results are presented for $y \geqslant 0$.

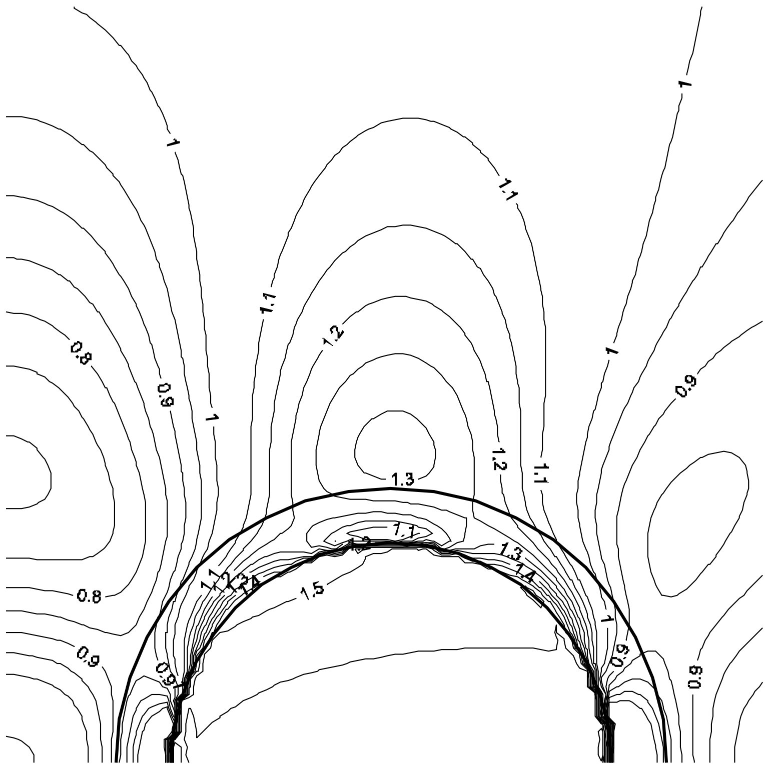

Fig. 6. Contours of $(\sigma_1 - \sigma_2)/\sigma_0$ for two perfectly bonded inclusions.

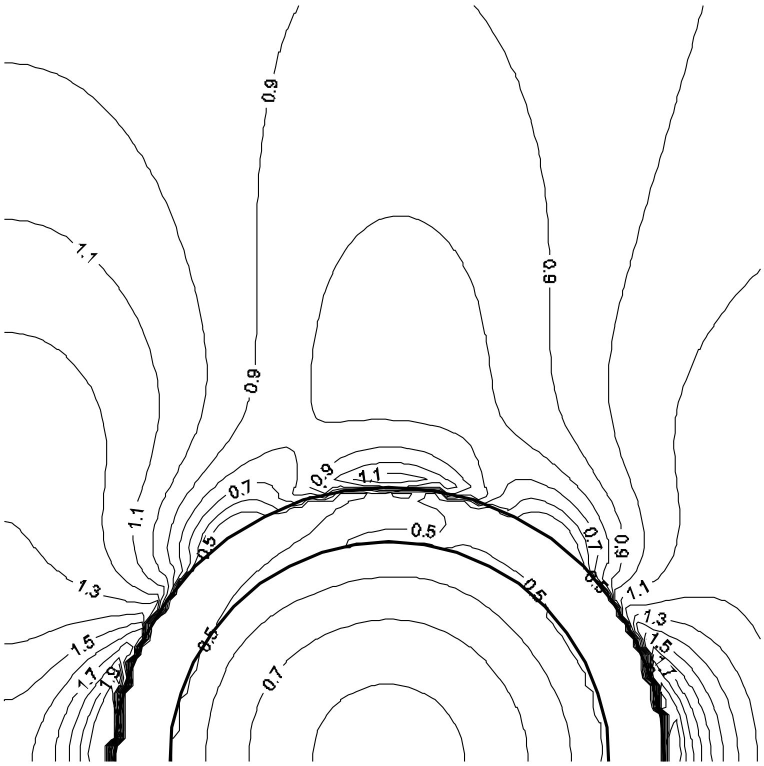

Fig. 7. Contours of $(\sigma_1 - \sigma_2)/\sigma_0$ for two inclusions with compliant coatings.

8.3. Equally spaced multiple inclusions

Consider a finite square array of $l \times l$ inclusions shown in Fig. 11. All the inclusions (fibers) have the same radii $R_{1j} = 8.5$ μm ($j = 1, \ldots, l$). The radii of the interphases are also all the same ($R_{2j} = 9.5$ μm). The volume fraction of the fibers is equal to 0.50 (the distances $2L$ between their centers are equal to 21.30634 μm). We take the elastic properties of the constituent materials as follows (we assume plane strain conditions and consider the case of four different Young's moduli for the interphases):

$$\begin{cases} E_{\text{fiber}} = 84.0 \text{ GPa}, \quad \nu_{\text{fiber}} = 0.22 \\ E_{\text{interphase}} = 4.0\text{–}12.0 \text{ GPa}, \quad \nu_{\text{interphase}} = 0.34 \\ E_{\text{matrix}} = 4.0 \text{ GPa}, \quad \nu_{\text{matrix}} = 0.34 \end{cases}$$

An infinite array with the same properties was considered by Wacker et al. (1998) (finite elements) and Liu et al. (2000) (boundary elements), who used a unit cell approach. These authors assumed macro-isotropic behavior of the equivalent homogeneous material (characterized by two elastic constants: effective Young's modulus E_{eff} and effective Poisson's ratio ν_{eff}) and studied the effect of variations in $E_{\text{interphase}}$ on E_{eff}. In the approach by Wacker et al., the boundary of the unit cell was subjected to displacement boundary conditions and E_{eff} was calculated using the fact that the strain energy of a composite material is equal to the strain energy of an equivalent homogeneous one. A mesh of 1834 linear triangular elements was used to model one quarter of a unit cell.

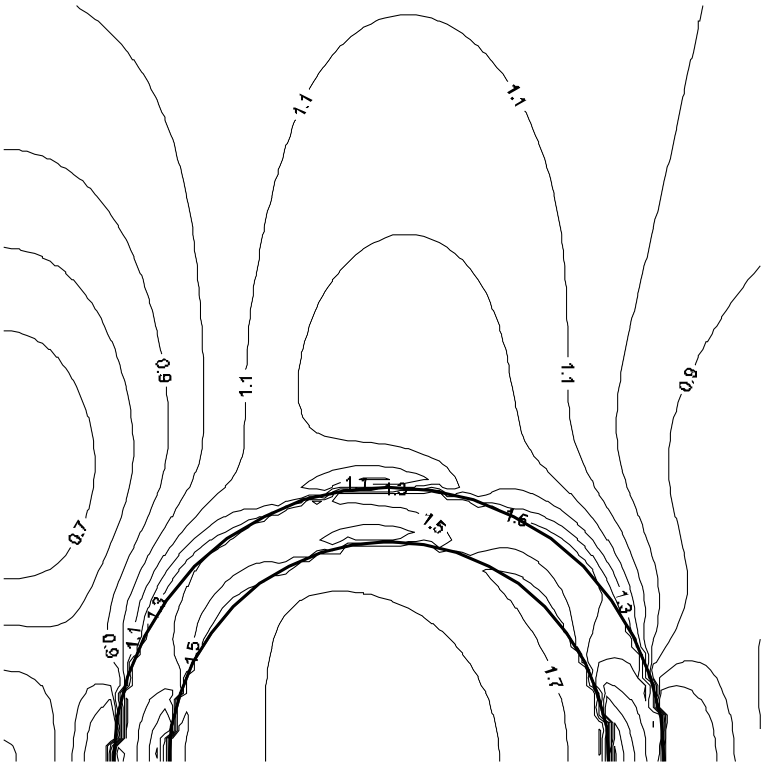

Fig. 8. Contours of $(\sigma_1 - \sigma_2)/\sigma_0$ for two inclusions with stiff coatings.

Liu et al. calculated E_{eff} from average stress–strain relations along the edge of a unit cell perpendicular to the direction of an applied uniaxial tension at infinity. They used two types of boundary conditions for the unit cell: *BEM 1*—traction free conditions ($\sigma_n = \sigma_s = 0$ along edges parallel to the applied remote tension) and *BEM 2*—straight line conditions (the edges parallel to the applied load remain straight after deformation). The boundary element mesh involved 64 quadratic boundary elements—16 elements for each circular boundary and 32 elements for the straight boundaries.

Taking different values of l, we used our approach to compute the stress and displacement distributions in the basic cell ($-L \leqslant x \leqslant L$, $-L \leqslant y \leqslant L$) of a finite array. Analysis of the displacement distribution along the boundaries of the basic cell showed that displacements at the edges parallel to the applied load were constant to within 4–6 digits when $l \geqslant 11$. The parameters δ_1 and δ_2 (Mogilevskaya and Crouch, 2001) for the Gauss–Seidel and external iterative algorithms were chosen as 10^{-6} and 10^{-3}, respectively. The algorithm converged within the specified accuracy with between 14 and 16 terms in the Fourier series, depending on the interphase properties. Using the assumption of macro-isotropic behavior of the equivalent homogeneous material we calculated the elastic constants of the equivalent homogeneous material. E_{eff} was calculated from average stress–strain relations along the edge $x = L$, $-L \leqslant y \leqslant L$. Table 2 shows the comparison between our results (with $l = 11$) and the ones obtained by Wacker et al. (1998) and Liu et al. (2000). Our results agree better with finite element ones.

Table 3 shows the variation of E_{eff} with the interphase properties (Young's modulus and thickness). It is worth mentioning that the interphase thickness does not introduce any singularity in the present approach. The number of terms in Fourier series remains of the same order as the interphase thickness decreases.

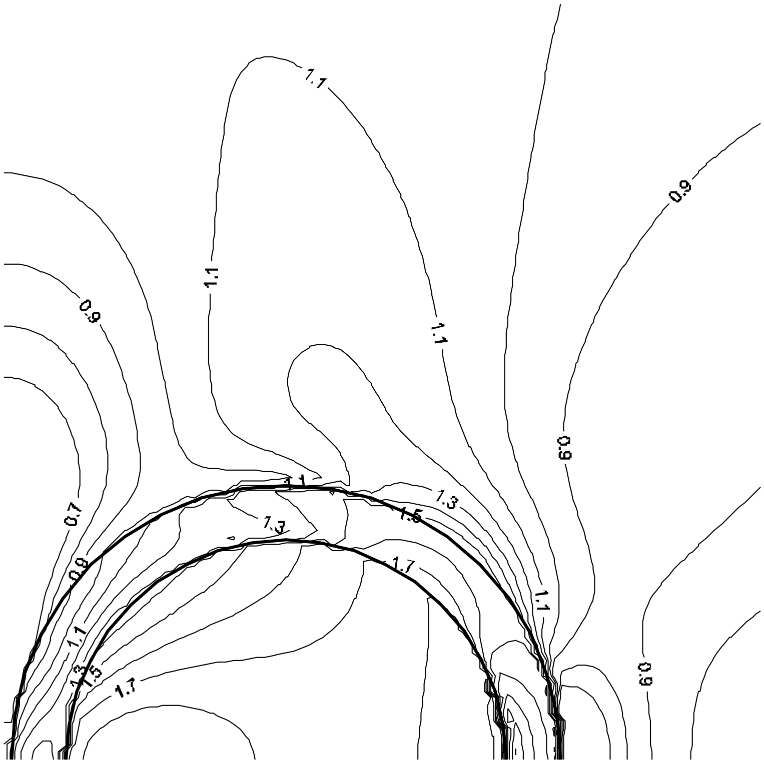

Fig. 9. Contours of $(\sigma_1 - \sigma_2)/\sigma_0$ for two close to touching inclusions with stiff coatings.

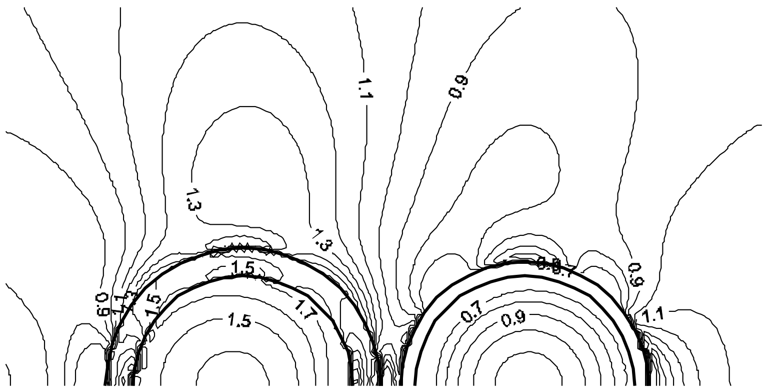

Fig. 10. Contours of $(\sigma_1 - \sigma_2)/\sigma_0$ for two inclusions with stiff (left) and compliant (right) coatings.

8.4. Random multiple inclusions

The final example shows the use of our approach for the solution of problems with multiple randomly distributed coated inclusions. Fig. 12 shows contours of $\sigma_1 - \sigma_2$ in a plane with 30 coated inclusions (volume

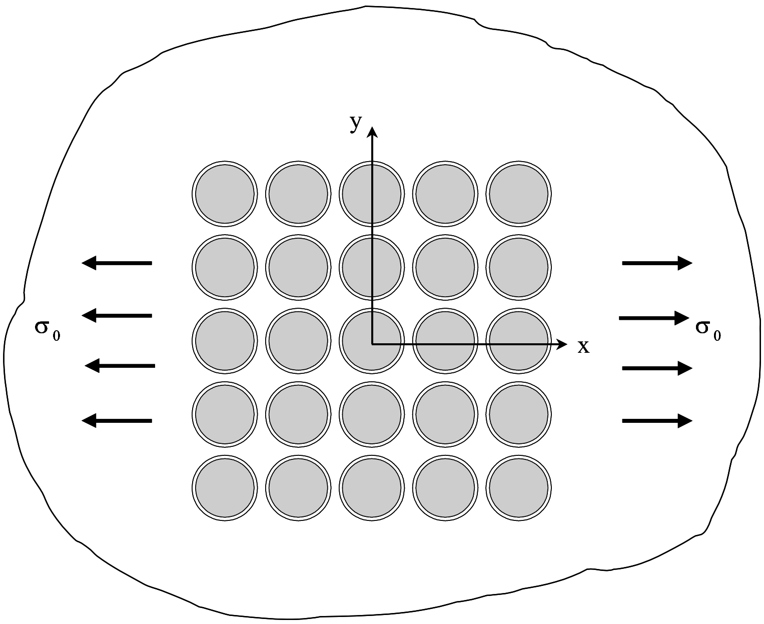

Fig. 11. Rectangular array of inclusions.

Table 2
Variation of E_{eff} with $E_{\text{interphase}}$ (comparison with BEM and FEM)

$E_{\text{interphase}}$ (GPa)	BEM 1	BEM 2	FEM	Current approach
4.0	11.61	11.61	12.25	12.09
6.0	13.18	13.02	13.71	13.68
8.0	13.97	13.89	14.68	14.67
12.0	15.04	14.93	15.91	15.84

Table 3
Variation of E_{eff} with the interphase properties ($E_{\text{interphase}}$ and $R_{2j} - R_{1j}$)

$E_{\text{interphase}}$ (GPa)	$R_{2j} - R_{1j}$ (μm)			
	1.0	0.5	0.1	0.01
4.0	12.09	12.09	12.09	12.09
6.0	13.68	12.86	12.24	12.10
8.0	14.67	13.29	12.32	12.11
12.0	15.84	13.76	12.40	12.12

fraction 0.53) subjected to uniform uniaxial tension $\sigma_{xx}^{\infty} = 1.0$. The Poisson's ratios of the inclusions, matrix, and the coatings are the same: $\nu_{\text{inclusion}} = \nu_{\text{matrix}} = \nu_{\text{coating}} = 0.2$. All the inclusions are stiff ($\mu_{\text{inclusion}}/\mu_{\text{matrix}} = 10$). Two types of coatings are present: stiff ($\mu_{\text{coating}}/\mu_{\text{matrix}} = 2$) for 23 inclusions and compliant ($\mu_{\text{coating}}/\mu_{\text{matrix}} = 0.5$) for 7. The numbers of terms in the Fourier series for the inclusions varied from 10 to 21 (with $\delta_1 = 10^{-6}$ and $\delta_2 = 10^{-3}$). The solution of this problem took less than a minute on a 2 GHz PC. The small number of the inclusions in this example was chosen merely to provide convenient visual

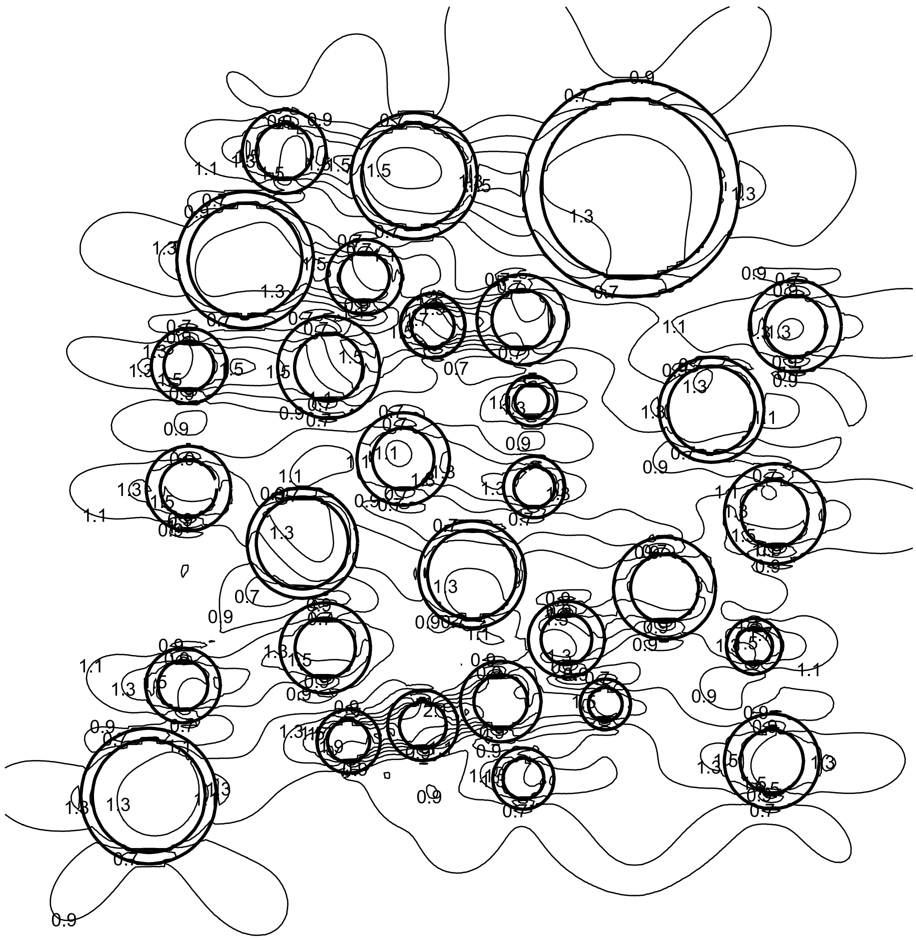

Fig. 12. Contours of $\sigma_1 - \sigma_2$ for 30 randomly distributed coated inclusions subjected to uniaxial tension at infinity ($\sigma_{xx}^{\infty} = 1.0$).

presentation of the results. The approach can be used to solve much more complicated problems with hundreds or thousands of inclusions.

9. Conclusions

In this paper we extend a recently developed numerical technique for solving the problem of an infinite elastic plane containing a large number of circular elastic inclusions to the case of inclusions with homogeneous uniform interphase layers. The method allows one to solve problems involving numerous inclusions with arbitrary elastic properties, sizes, and interphase thicknesses. The only restrictions are that the interphases (and inclusions) may not overlap and that perfect bonding is assumed to exist between the interphases, the inclusions, and the material matrix. The test results obtained with the approach agree well with analytical and numerical solutions available in the literature. The main advantage of the approach is that apart from round-off the only errors introduced into the solution are due to truncation of the Fourier series used to approximate the unknown tractions at the inclusion–interphase and interphase–matrix boundaries. Compared to finite element and boundary element solutions of similar problems, our approach requires relatively few of degrees of freedom to model inclusions with very thin interphases. It is shown that the problem of overlapping of fibers and matrix, though not completely eliminated in present model, can be attributed to rather extreme interphase conditions. Natural future developments of the approach include the extension to problems with radially graded interphases.

Appendix A. Stresses at internal points

Using the notation

$$\begin{aligned}\Sigma_{1kj}(z) &= a_{1kj}\sum_{m=2}^{M_j} B_{-mkj}F_{mkj}(z)\\ \Sigma_{2kj}(z) &= B_{0kj}(a_{3kj}-2a_{1kj})F_{2kj}(z) + a_{1kj}\sum_{m=2}^{M_j} B_{-mkj}\left[\frac{mF_{(m+1)kj}(z)}{\overline{F_{1kj}(z)}} - (m+1)F_{(m+2)kj}(z)\right]\\ &\quad + (a_{3kj}-a_{1kj})\sum_{m=1}^{M_j}\overline{B}_{mkj}F_{(m+2)kj}(z)\end{aligned} \tag{A.1}$$

it can be shown that the stresses inside the ℓth inclusion are

$$\begin{aligned}(\sigma_{xx})_\ell + (\sigma_{yy})_\ell &= \frac{8\mu_{1\ell}}{\kappa_{1\ell}+1}\mathrm{Re}\sum_{k=1}^{2}\left[a_{1k\ell}\sum_{m=0}^{M_\ell} B_{mk\ell}/F_{mk\ell}(z) - \sum_{\substack{j=1\\ j\neq\ell}}^{N}\Sigma_{1kj}(z)\right]\\ &\quad + \frac{\mu_{1\ell}(\kappa+1)}{\mu(\kappa_{1\ell}+1)}\left(\sigma_{xx}^\infty + \sigma_{yy}^\infty\right)\\ (\sigma_{yy})_\ell - (\sigma_{xx})_\ell + 2\mathrm{i}(\sigma_{xy})_\ell &= \frac{4\mu_{1\ell}}{\kappa_{1\ell}+1}\sum_{k=1}^{2}\left\{a_{1k\ell}\sum_{m=1}^{M_\ell} B_{mk\ell}\left[\frac{m}{F_{(m-1)k\ell}(z)\overline{F_{1k\ell}(z)}} - \frac{m-1}{F_{(m-2)k\ell}(z)}\right]\right.\\ &\quad \left. + (a_{1k\ell}-a_{3k\ell})\sum_{m=2}^{M_\ell}\overline{B}_{-mk\ell}/F_{(m-2)k\ell}(z) + \sum_{\substack{j=1\\ j\neq\ell}}^{N}\Sigma_{2kj}(z)\right\}\\ &\quad + \frac{\mu_{1\ell}(\kappa+1)}{\mu(\kappa_{1\ell}+1)}\left(\sigma_{yy}^\infty - \sigma_{xx}^\infty + 2\mathrm{i}\sigma_{xy}^\infty\right)\end{aligned} \tag{A.2}$$

the stresses inside the ℓth interphase are

$$\begin{aligned}(\sigma_{xx})_\ell + (\sigma_{yy})_\ell &= -\frac{8\mu_{2\ell}}{\kappa_{2\ell}+1}\mathrm{Re}\left[a_{11\ell}\sum_{m=2}^{M_\ell} B_{-m1\ell}F_{m1\ell}(z) - a_{12\ell}\sum_{m=0}^{M_\ell} B_{m2\ell}/F_{m2\ell}(z)\right.\\ &\quad \left. + \sum_{k=1}^{2}\sum_{\substack{j=1\\ j\neq\ell}}^{N}\Sigma_{1kj}(z)\right] + \frac{\mu_{2\ell}(\kappa+1)}{\mu(\kappa_{2\ell}+1)}\left(\sigma_{xx}^\infty + \sigma_{yy}^\infty\right)\end{aligned}$$

$$(\sigma_{yy})_\ell - (\sigma_{xx})_\ell + 2\mathrm{i}(\sigma_{xy})_\ell = \frac{4\mu_{2\ell}}{\kappa_{2\ell}+1}\left\{ B_{01\ell}(a_{31\ell} - 2a_{11\ell})F_{21\ell}(z) + a_{11\ell}\sum_{m=2}^{M_\ell} B_{-m1\ell}\left[\frac{mF_{(m+1)1\ell}(z)}{\overline{F_{11\ell}(z)}} - (m+1)F_{(m+2)1\ell}(z)\right] + (a_{31\ell} - a_{11\ell})\sum_{m=1}^{M_\ell} \overline{B}_{m1\ell}F_{(m+2)1\ell}(z) + a_{12\ell}\sum_{m=1}^{M_\ell} B_{m2\ell}\left[\frac{m}{F_{(m-1)2\ell}(z)\overline{F_{12\ell}(z)}} - \frac{m-1}{F_{(m-2)2\ell}(z)}\right] + \sum_{k=1}^{2}\sum_{\substack{j=1\\ j\neq\ell}}^{N} \Sigma_{2kj}(z)\right\} + \frac{\mu_{2\ell}(\kappa+1)}{\mu(\kappa_{2\ell}+1)}\left(\sigma_{yy}^\infty - \sigma_{xx}^\infty + 2\mathrm{i}\sigma_{xy}^\infty\right) \tag{A.3}$$

and the stresses σ_{xx}, σ_{yy}, and σ_{xy} in the matrix are

$$\begin{aligned} \sigma_{xx} + \sigma_{yy} &= -\frac{8\mu}{\kappa+1}\mathrm{Re}\sum_{k=1}^{2}\sum_{j=1}^{N}\Sigma_{1kj}(z) + \left(\sigma_{xx}^\infty + \sigma_{yy}^\infty\right) \\ \sigma_{yy} - \sigma_{xx} + 2\mathrm{i}\sigma_{xy} &= \frac{4\mu}{\kappa+1}\sum_{k=1}^{2}\sum_{j=1}^{N}\Sigma_{2kj}(z) + \left(\sigma_{yy}^\infty - \sigma_{xx}^\infty + 2\mathrm{i}\sigma_{xy}^\infty\right) \end{aligned} \tag{A.4}$$

Appendix B. Displacements at internal points

Using the notation

$$G_{p\ell} = \sum_{k=1}^{2}\sum_{\substack{j=1\\ j\neq\ell}}^{N}\left[B_{0kj}(a_{3kj} - 2a_{1kj})R_{kj}\overline{F_{1kj}(z_\ell)} - a_{1kj}\sum_{m=2}^{M_j} B_{-mkj}\frac{F_{(m-1)kj}(z_\ell)}{m-1} - a_{1kj}\sum_{m=2}^{M_j}\overline{B}_{-mkj}\overline{F_{(m-1)kj}(z_\ell)}\left(\overline{F_{2kj}(z_\ell)} + m\overline{F_{2p\ell}(z_j)} - \frac{z_\ell - z_j}{\overline{z}_\ell - \overline{z}_j}\right) + (a_{3kj} - a_{1kj})\sum_{m=1}^{M_j} B_{mkj}\frac{\overline{F_{(m+1)kj}(z_\ell)}}{m+1}\right] - \frac{\kappa+1}{4\mu}\left(\sigma_{xx}^\infty + \sigma_{yy}^\infty\right)z_\ell - \frac{\kappa+1}{4\mu}\left(\sigma_{yy}^\infty - \sigma_{xx}^\infty - 2\mathrm{i}\sigma_{xy}^\infty\right)\overline{z_\ell} \tag{B.1}$$

and

$$\Lambda_{kj}(z,\kappa_\ell) = B_{0kj}(a_{3kj} - 2a_{1kj})R_{kj}\overline{F_{1kj}(z)} + \kappa_\ell a_{1kj}\sum_{m=2}^{M_j} B_{-mkj}\frac{z - z_j}{m-1}F_{mkj}(z) + a_{1kj}\sum_{m=2}^{M_j}\overline{B}_{-mkj}\overline{F_{(m+1)kj}(z)}\frac{(z - z_j) - R_{kj}\overline{F_{1kj}(z)}}{\overline{F_{1kj}(z)}} + (a_{3kj} - a_{1kj})R_{kj}\sum_{m=1}^{M_j} B_{mkj}\frac{\overline{F_{(m+1)kj}(z)}}{m+1} \tag{B.2}$$

it can be shown that the displacements inside the ℓth inclusion are

$$u(z)=\frac{1}{\kappa_{1\ell}+1}\sum_{k=1}^{2}\Bigg\{a_{1k\ell}\Bigg[B_{0k\ell}(\kappa_{1\ell}-1)(z-z_\ell)+\kappa_{1\ell}R_{k\ell}\sum_{m=1}^{M_\ell}B_{mk\ell}\frac{1}{(m+1)F_{(m+1)k\ell}(z)}$$

$$+\sum_{m=1}^{M_\ell}\overline{B}_{mk\ell}\frac{R_{k\ell}\overline{F_{1k\ell}(z)}-(z-z_\ell)}{\overline{F_{mk\ell}(z)}}\Bigg]+(a_{3k\ell}-a_{1k\ell})R_{k\ell}\sum_{m=2}^{M_\ell}B_{-mk\ell}\frac{1}{(m-1)\overline{F_{(m-1)k\ell}(z)}}+\sum_{\substack{j=1\\j\neq\ell}}^{N}\Lambda_{kj}(z,\kappa_{1\ell})\Bigg\}$$

$$+\frac{(\kappa_{1\ell}-1)(\kappa+1)}{8\mu(\kappa_{1\ell}+1)}\left(\sigma_{xx}^{\infty}+\sigma_{yy}^{\infty}\right)z-\frac{\kappa+1}{4\mu(\kappa_{1\ell}+1)}\left(\sigma_{yy}^{\infty}-\sigma_{xx}^{\infty}-2\mathrm{i}\sigma_{xy}^{\infty}\right)\overline{z}$$

$$+\left(\frac{1}{\kappa_{2\ell}+1}-\frac{1}{\kappa_{1\ell}+1}\right)\left[a_{12\ell}\overline{B}_{12\ell}R_{2\ell}\left(1-\frac{R_{1\ell}^2}{R_{2\ell}^2}\right)+G_{1\ell}\right]+\left(\frac{1}{\kappa+1}-\frac{1}{\kappa_{2\ell}+1}\right)G_{2\ell}$$

the displacements inside the ℓth interphase are

$$u(z)=\frac{1}{\kappa_{2\ell}+1}\Bigg\{(a_{31\ell}-2a_{11\ell})B_{01\ell}R_{1\ell}\overline{F_{11\ell}(z)}+a_{12\ell}(\kappa_{2\ell}-1)B_{02\ell}(z-z_\ell)+a_{11\ell}\kappa_{2\ell}R_{1\ell}\sum_{m=2}^{M_\ell}B_{-m1\ell}\frac{F_{(m-1)1\ell}(z)}{m-1}$$

$$+a_{12\ell}\kappa_{2\ell}R_{2\ell}\sum_{m=1}^{M_\ell}B_{m2\ell}\frac{1}{(m+1)F_{(m+1)2\ell}(z)}-a_{11\ell}\sum_{m=2}^{M_\ell}\overline{B}_{-m1\ell}\frac{R_{1\ell}\overline{F_{11\ell}(z)}-(z-z_\ell)}{\overline{F_{11\ell}(z)}}\overline{F_{(m+1)1\ell}(z)}$$

$$+a_{12\ell}\sum_{m=1}^{M_\ell}\overline{B}_{m2\ell}\frac{R_{2\ell}\overline{F_{12\ell}(z)}-(z-z_\ell)}{\overline{F_{m2\ell}(z)}}+(a_{31\ell}-a_{11\ell})R_{1\ell}\sum_{m=1}^{M_\ell}B_{m1\ell}\frac{\overline{F_{(m+1)1\ell}(z)}}{m+1}$$

$$+(a_{32\ell}-a_{12\ell})R_{2\ell}\sum_{m=2}^{M_\ell}B_{-m2\ell}\frac{1}{(m-1)\overline{F_{(m-1)2\ell}(z)}}+\sum_{k=1}^{2}\sum_{\substack{j=1\\j\neq\ell}}^{N}\Lambda_{kj}(z,\kappa_{2\ell})\Bigg\}$$

$$+\frac{(\kappa_{2\ell}-1)(\kappa+1)}{8\mu(\kappa_{2\ell}+1)}\left(\sigma_{xx}^{\infty}+\sigma_{yy}^{\infty}\right)z-\frac{\kappa+1}{4\mu(\kappa_{2\ell}+1)}\left(\sigma_{yy}^{\infty}-\sigma_{xx}^{\infty}-2\mathrm{i}\sigma_{xy}^{\infty}\right)\overline{z}+\left(\frac{1}{\kappa+1}-\frac{1}{\kappa_{2\ell}+1}\right)G_{2\ell}$$

and the displacements in the matrix are

$$u(z)=\frac{1}{\kappa+1}\sum_{k=1}^{2}\sum_{j=1}^{N}\Lambda_{kj}(z,\kappa)+\frac{(\kappa-1)}{8\mu}\left(\sigma_{xx}^{\infty}+\sigma_{yy}^{\infty}\right)z-\frac{1}{4\mu}\left(\sigma_{yy}^{\infty}-\sigma_{xx}^{\infty}-2\mathrm{i}\sigma_{xy}^{\infty}\right)\overline{z}$$

References

Aboudi, J., 1987. Damage in composites—Modeling of imperfect bonding. Composites Science and Technology 28, 103–128.

Achenbach, J.D., Zhu, H., 1989. Effect of interfacial zone on mechanical behavior and failure of fiber-reinforced composites. Journal of the Mechanics and Physics of Solids 37, 381–393.

Achenbach, J.D., Zhu, H., 1990. Effect of interphases on micro and macromechanical behavior of hexagonal-array fiber composites. Journal of Applied Mechanics 57, 956–963.

Al-Ostaz, A., Jasiuk, I., 1996. The influence of interface and arrangement of inclusions on local stresses in composite materials. Acta Materialia 45, 4131–4143.

Benveniste, Y., Miloh, T., 2001. Imperfect soft and stiff interfaces in two-dimensional elasticity. Mechanics of Materials 33, 309–323.

Benveniste, Y., Dvorak, G.J., Chen, T., 1989. Stress fields in composites with coated inclusions. Mechanics of Materials 7, 305–317.

Bigoni, D., Movchan, A.B., 2002. Statics and dynamics of structural interfaces in elasticity. International Journal of Solids and Structures 39, 4843–4865.

Bigoni, D., Serkov, S.K., Valentini, M., Movchan, A.B., 1998. Asymptotic models of dilute composites with imperfectly bonded inclusions. International Journal of Solids and Structures 35, 3239–3258.

Brebbia, C.A., Telles, J.C.F., Wrobel, L.C., 1984. Boundary Element Techniques: Theory and Applications in Engineering. Springer-Verlag, Berlin, Heidelberg, New-York, Tokyo.

Christensen, R.M., Lo, K.H., 1979. Solutions for effective shear properties in three phase sphere and cylinder models. Journal of the Mechanics and Physics of Solids 27, 315–330.

Crasto, A.S., Own, S.H., Subramanian, R.V., 1988. The influence of the interphase on composite properties: poly(ethylene-co-acrylic acid) and poly(methyl vinyl ether-co-maleic anhydride) electrodeposited on graphite fibers. Polymer Composites 9, 78–92.

Crouch, S.L., Mogilevskaya, S.G., 2003. On the use of Somigliana's formula and Fourier series for elasticity problems with circular boundaries. International Journal for Numerical Methods in Engineering 58, 537–578.

Golub, G.H., Van Loan, C.F., 1996. Matrix Computation. J. Hopkins University Press, Baltimore, London.

Gulrajani, S.N., Mukherjee, S., 1993. Sensitivities and optimal design of hexagonal array fiber composites with respect to interphase properties. International Journal of Solids and Structures 30, 2009–2026.

Hashin, Z., 1990. Thermoelastic properties of fiber composites with imperfect interface. Mechanics of Materials 8, 333–348.

Hashin, Z., 1991. Thermoelastic properties of particulate composites with imperfect interface. Journal of the Mechanics and Physics of Solids 39, 745–762.

Hashin, Z., 2002. Thin interphase/imperfect interface in elasticity with application to coated fiber composites. Journal of the Mechanics and Physics of Solids 50, 2509–2537.

Jasiuk, I., Kouider, M.W., 1993. The effect of an inhomogeneous interphase on the elastic constants of transversely isotropic composites. Mechanics of Materials 15, 53–63.

Kouris, D., 1993. Stress concentration due to the interaction between two imperfectly bonded fibers in a continuous fiber composite. Journal of Applied Mechanics 60, 203–206.

Lagache, M., Agbossou, A., Pastor, J., 1994. Role of interphase on the elastic behavior of composite materials: theoretical and experimental analysis. Journal of composite materials 28, 1140–1157.

Linkov, A.M., Mogilevskaya, S.G., 1994. Complex hypersingular integrals and integral equations in plane elasticity. Acta Mechanica 105, 189–205.

Liu, Y.J., Xu, N., Luo, J.F., 2000. Modeling of interphases in fiber-reinforced composites under transverse loading using the boundary element method. Journal of Applied Mechanics 67, 41–49.

Lutz, M.P., Zimmerman, R.W., 1996. Effect of the interphase zone on the bulk modulus of a particulate composite. Journal of Applied Mechanics 63, 855–861.

Mascia, L., Dhillon, J., Harper, J.F., 1993. Adhesion enhancement of rubbery and ductile polyolefin coatings on glass fibers for epoxy composites and effect on failure mechanism. Journal of Applied Polymer Science 47, 487–498.

Mogilevskaya, S.G., Crouch, S.L., 2001. A Galerkin boundary integral method for multiple circular elastic inclusions. International Journal for Numerical Methods in Engineering 52, 1069–1106.

Mogilevskaya, S.G., Crouch, S.L., 2002. A Galerkin boundary integral method for multiple circular elastic inclusions with homogeneously imperfect interfaces. International Journal of Solids and Structures 39, 4723–4746 (Erratum in International Journal of Solids and Structures 40, 1335).

Muskhelishvili, N.I., 1959. Some Basic Problems of the Mathematical Theory of Elasticity. Noordhoff, Groningen, The Netherlands.

Nassehi, V., Dhillon, J., Mascia, L., 1993a. Finite element simulation of the micromechanics of interlayered polymer/fibre composites: a study of the interactions between the reinforcing phases. Composites Science and Technology 47, 349–358.

Nassehi, V., Kinsella, M., Mascia, L., 1993b. Finite element modelling of the stress distribution in polymer composites with coated fibre interlayers. Journal of Composite Materials 27, 195–214.

Pan, L., Adams, D.O., Rizzo, F.J., 1998. Boundary element analysis for composite materials and a library of Green's functions. Computers and Structures 66, 685–693.

Ru, C.Q., 1998. A circular inclusion with circumferentially inhomogeneous sliding interface in plane elastostatics. Journal of Applied Mechanics 65, 30–38.

Ru, C.Q., 1999. A new method for an inhomogeneity with stepwise graded interphase under thermomechanical loadings. Journal of Elasticity 56, 107–127.

Ru, C.Q., Schiavone, P., 1997. A circular inclusion with circumferentially inhomogeneous interface in antiplane shear. Proceedings of the Royal Society of London A 453, 2551–2572.

Sudak, L.J., Mioduchowski, A., 2002. A three-phase circular inhomogeneity with imperfect interface under thermomechanical loadings in plane elasticity. Acta Mechanica 158, 43–56.

Sudak, L.J., Ru, C.Q., Schiavone, P., Mioduchowski, A., 1999. A circular inclusion with inhomogeneously imperfect interface in plane elasticity. Journal of Elasticity 55, 19–41.

Subramanian, R.V., Crasto, A.S., 1986. Electrodeposition of a polymer interphase in carbon-fiber composites. Polymer Composites 7, 201–218.

Theocaris, P.S., 1987. The Mesophase Concept in Composites. Springer-Verlag, New York.

Wacker, G., Bledzki, A.K., Chate, A., 1998. Effect of interphase on the trasverse Young's modulus of glass/epoxy composites. Composites 29A, 619–626.

Wang, J., Crouch, S.L., Mogilevskaya, S.G., 2003. A complex boundary integral method for multiple circular holes in an infinite plane. Engineering Analysis with Boundary Elements 27, 789–802.

Wang, J., Mogilevskaya, S.G., Crouch, S.L. A numerical procedure for multiple circular holes and elastic inclusions in a finite domain with a circular boundary. Computational Mechanics, in press.

Zhu, H., Achenbach, J.D., 1991. Radial matrix cracking and interphase failure in transversely loaded fiber composites. Mechanics of Materials 11, 347–356.